The Canadian Mineralogist
Vol. 33, pp. 793-815 (1995)

THE RARE-ELEMENT-ENRICHED MONZOGRANITE – PEGMATITE – QUARTZ VEIN SYSTEMS IN THE PREISSAC–LACORNE BATHOLITH, QUEBEC. I. GEOLOGY AND MINERALOGY

THOMAS MULJA, ANTHONY E. WILLIAMS-JONES, SCOTT A. WOOD[1] AND MICHEL BOILY[2]
Department of Earth and Planetary Sciences, McGill University, 3450 University Street, Montreal, Quebec H3A 2A7

ABSTRACT

The monzogranitic plutons in the Preissac–Lacorne batholith, Quebec, in the Abitibi Greenstone Belt of the Superior Province, display geological and mineralogical features that resemble idealized zoned intrusions and associated rare-element pegmatites and quartz veins. The zoning comprises biotite, two-mica, and muscovite monzogranites; the mineralization in pegmatite-poor plutons is dominated by molybdenite-bearing quartz veins, which are spatially related to the more evolved rocks (*i.e.*, muscovite-bearing monzogranite). In contrast, pegmatite-rich plutons are surrounded by rare-element pegmatites, which vary systematically with distance from the plutons from beryl-bearing through spodumene–beryl-bearing to spodumene-bearing. In addition, Mo-bearing albitite dikes and quartz veins occur beyond the spodumene pegmatites. Mineralogical changes from biotite to muscovite monzogranite are characterized by a decrease in the abundance of oligoclase, biotite, magnetite, monazite, apatite, and zircon, and an increase in the abundance of albite, muscovite and garnet. The mineralogical trend continues into the pegmatites, which are composed of albite, K-feldspar, quartz, muscovite (biotite is absent), garnet, beryl, spodumene, molybdenite, and columbite–tantalite. The major-element chemistry of the rock-forming minerals changes progressively from biotite through two-mica to muscovite monzogranite; plagioclase compositions vary from An_{13-17} to An_6, and the Fe/(Fe + Mg) of biotite and muscovite increases from 0.7 to 0.85 and from 0.65 to 0.85, respectively. This mineral-chemical evolution extends into the pegmatites; the plagioclase in these rocks is almost pure albite (An_{1-5}), and muscovite is lower in Fe/(Fe + Mg) and richer in Al than that in the muscovite monzogranite. Concentrations of Cs, Ta, and Rb in muscovite increase, whereas that of Sc decreases, from the muscovite monzogranite to the rare-metal pegmatites. The systematic mineralogical evolution and mineral-chemical trends, and the field relationships of the monzogranites, are interpreted to indicate that the various subtypes of monzogranite were produced mainly by fractional crystallization of biotite monzogranitic magma. Further differentiation of the fractionated monzogranitic melts produced rare-element pegmatites.

Keywords: rare-element monzogranite, beryl pegmatite, spodumene pegmatite, mineralogy, mineral chemistry, Preissac–Lacorne batholith, Quebec.

SOMMAIRE

Les plutons monzogranitiques du batholite de Preissac–Lacorne, dans la ceinture de roches vertes de l'Abitibi, province du Supérieur (Québec), démontrent des critères géologiques et minéralogiques d'une séquence idéale d'un massif intrusif zoné, avec cortège de veines de quartz et de pegmatites granitiques enrichies en éléments rares. On peut y distinguer des monzogranites à biotite, à deux micas et à muscovite. La minéralisation dans les plutons à faible représentation de pegmatites se manifeste surtout par des veines de quartz avec molybdénite. Celles-ci sont liées dans l'espace aux roches plutoniques les plus évoluées (monzogranite à muscovite). Par contre, les plutons à forte représentation de pegmatites sont entourés de filons de pegmatite dont la constitution minéralogique change avec distance du pluton parent, de pegmatite à béryl, à pegmatite à béryl + spodumène, jusqu'au faciès à spodumène. De plus, nous décrivons des filons d'albitite à molybdénite et des veines de quartz au delà des pegmatites à spodumène. En passant du monzogranite à biotite au monzogranite à muscovite, on voit une diminution dans la proportion de l'oligoclase, la biotite, la magnétite, la monazite, l'apatite et le zircon, et une augmentation dans la proportion de l'albite, la muscovite et le grenat. Ces changements continuent en passant aux pegmatites, qui sont faites d'albite, de feldspath potassique, de quartz et de muscovite (la biotite est absente), avec grenat, béryl, spodumène, molybdénite, et columbite–tantalite. La composition des minéraux majeurs change de façon continue d'un faciès du monzogranite à l'autre. Le plagioclase passe de An_{13-17} à An_6, et le rapport Fe/(Fe + Mg) de la biotite et de la muscovite augmente de 0.7 à 0.85 et de 0.65 à 0.85, respectivement. Dans les pegamtites, le plagioclase est presque de l'albite pure (An_{1-5}), et la muscovite a un rapport Fe/(Fe + Mg) plus faible et est plus fortement alumineuse que dans le monzogranite à muscovite. Les concentrations de Cs, Ta et Rb dans la muscovite augmentent, tandis que la teneur en Sc diminue, en passant du monzogranite à muscovite aux pegmatites enrichis en éléments rares. Les transitions systématiques dans la minéralogie et la composition chimique des minéraux dans les divers faciès résulteraient d'une cristallisation fractionnée d'un magma monzogranitique. Une différenciation plus poussée des liquides monzogranitiques évolués est responsable de la formation des pegmatites enrichis en éléments rares.

(Traduit par la Rédaction)

Mots-clés: monzogranite à éléments rares, pegmatite à béryl, pegmatite à spodumène, minéralogie, composition des minéraux, batholite de Preissac–Lacorne, Québec.

---

[1] Present address: Department of Geology and Geological Engineering, University of Idaho, Moscow, Idaho 83843, U.S.A.
[2] Present address: Géon, 10785, rue St-Urbain, Montréal, Québec H3L 2V4.

Introduction

Petrologically zoned rare-metal (*e.g.*, Be, Li, Nb, Ta, Sn)-enriched granitic intrusions have been described by a number of investigators, and a model has been developed in which fractional crystallization of a biotite-bearing monzogranitic melt gives rise to successive residual melts that crystallize to two-mica and muscovite monzogranites, and rare-metal pegmatites (*e.g.*, Goad & Černý 1981, Černý *et al.* 1986, Shearer *et al.* 1987, 1992, Simmons *et al.* 1987, Breaks & Moore 1992). However, there are few examples where all the model facies are exposed. Consequently, details of the process of differentiation have been poorly documented, and the specific factors responsible for the concentration of the rare metals to economic levels remain largely unknown.

The Preissac–Lacorne batholith hosts well-exposed monzogranitic plutons, which vary systematically from a least- evolved biotite monzogranite, through a two-mica, to a most evolved muscovite monzogranite, and are associated with rare-metal-enriched pegmatites, albitites, and molybdenite-bearing quartz veins. These plutons thus afford an unusually fine opportunity to investigate the causes of zonation of rare-metal-bearing monzogranites, the petrogenetic relationships between the monzogranites and the later pegmatites, albitites and quartz veins, and the rare-metal enrichment processes. In this paper we discuss the geology, mineralogy and mineral-chemical evolution of the monzogranitic plutons and associated pegmatites, and the physical conditions of emplacement of the intrusion. In the companion paper (Mulja *et al.* 1995b), we document the geochemical evolution of the plutons and evaluate the genetic relationship of the pegmatites to the monzogranites.

Geological Setting

The Preissac–Lacorne batholith, located about 600 km northwest of Montréal (Fig. 1), is a syn- to post-tectonic intrusion that was emplaced in the Southern Volcanic Zone of the Archean Abitibi Greenstone Belt, in the Superior Province of the Canadian Shield. Previous work, especially that of Dawson (1966), has established that the batholith intruded along the La Pause anticline into ultramafic to basic lavas of the Kinojevis (2718 Ma; Corfu 1993) and Malartic groups, and biotite schist of the Kewagama Group. To the north, the batholith is bounded by the Manneville fault, and to the south, by the Cadillac fault and the eastward extension of the Porcupine–Destor fault, which separates the batholith from rocks of the Pontiac Subprovince to the south. Gravity measurements indicate that the shape of the batholith resembles an outward-dipping, asymmetrical saddle with its highest points south of the center of the body, and suggest that the base of the batholith is probably at a depth of about 5 km (Dawson 1966).

The batholith is a composite body (Fig. 1), comprising early metaluminous gabbro, diorite, monzonite and granodiorite (*ca.* 2650–2760 Ma: Steiger & Wasserburg 1969, Feng & Kerrich 1991), and four late peraluminous monzogranitic plutons (Preissac, Moly Hill, Lamotte, and Lacorne) and associated pegmatites and quartz veins (*ca.* 2621–2655 Ma: Gariépy & Allègre 1985, Feng & Kerrich 1991). Intrusive activity in the region terminated with the emplacement of northeast-trending Proterozic diabase dikes. The regional metamorphic grade is greenschist facies, and in the vicinity of the batholith, mineral assemblages indicate contact-metamorphic conditions consistent with hornblende hornfels facies. Powell *et al.* (1994) mapped biotite, actinolite, hornblende and garnet isograds around the batholith. Using garnet – muscovite – biotite – plagioclase geothermobarometry and multi-equilibrium calculations based on assemblages of metamorphic minerals, they estimated the pressure–temperature conditions of contact metamorphism to be 3.5 kbar, and up to 450°C, respectively.

The Preissac–Lacorne batholith is believed to have formed during the waning stages of the development of the Abitibi Greenstone Belt (Dimroth *et al.* 1983, Feng & Kerrich 1992, Sutcliffe *et al.* 1993), which involved the collision of continents in a convergent plate setting. The basic igneous rocks in the batholith are interpreted to be products of partial melting of a mantle wedge above a subduction zone, and the monzogranites, to be products of partial melting of the sedimentary rocks of the Pontiac Subprovince (*e.g.*, greywacke), induced by crustal thickening associated with the collision of the Pontiac Subprovince with the Southern Volcanic Zone of the Abitibi Greenstone Belt.

Field Relationships and Petrography of the Monzogranite

Our detailed mapping and petrography indicate that the monzogranite is mineralogically and geologically divisible into biotite, two-mica, and muscovite subtypes (Figs. 2A–D). Biotite monzogranite is distinguished from the other types of monzogranite by the presence of up to 5 vol.% biotite and by the lack of primary muscovite. The two-mica monzogranite has a preponderance of muscovite over biotite (2:1), and the muscovite monzogranite contains little or no biotite. In the case of the Preissac pluton, there is an additional variant of monzogranite that occurs as fine-grained dikes, and differs from the other monzogranites by containing up to 3 vol.% garnet, 5 vol.% muscovite, and no biotite.

All the subtypes of monzogranite have similar proportions of interlocking anhedral quartz (25–35%), euhedral to subhedral plagioclase (30–45%), and

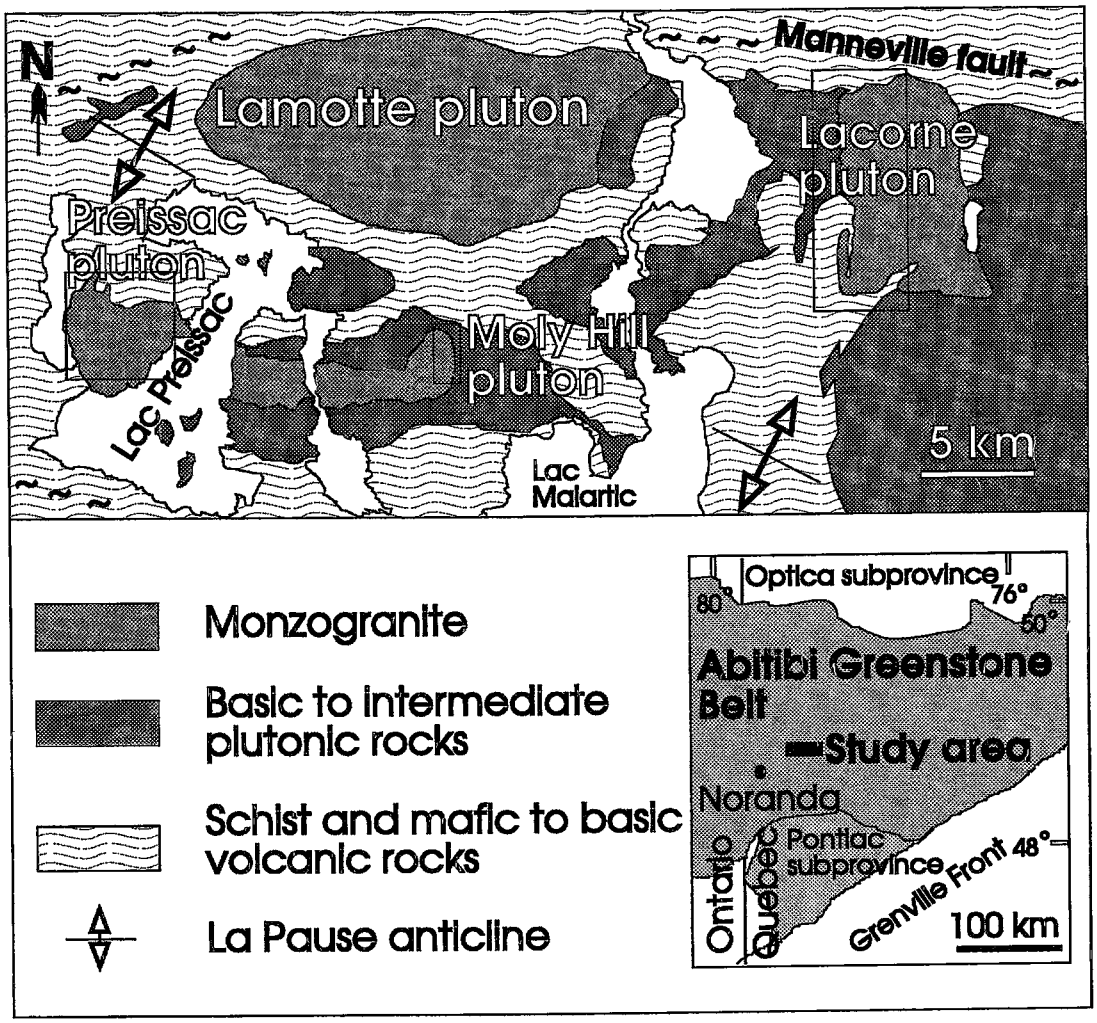

FIG. 1. A simplified geological map of the Preissac–Lacorne batholith (modified from Dawson 1966) showing the locations of monzogranitic plutons and regional structures. The Porcupine–Destor fault is located south of Lac Preissac and joins the east–west-trending Cadillac fault further south. The boundaries of the plutons are based on the outermost occurrence of small, scattered outcrops of monzogranite. The basic and intermediate plutonic rocks (gabbro, diorite, monzonite and granodiorite) are believed to extend as far as 10 km east and 15 km south of the Lacorne pluton.

perthitic to microperthitic K-feldspar (25–45%). Plagioclase is the earliest major mineral to have crystallized; inclusions of this mineral are present in K-feldspar. Plagioclase grains in biotite monzogranite have a corroded core with sericite flakes, and resemble restite plagioclase described by Chappell *et al.* (1987). However, this "restite" interpretation has been challenged by Wall et al. (1987), who argued that such corroded cores could represent formerly high-temperature calcic plagioclase that became unstable as the magma cooled. Moreover, geochemical evidence (Mulja *et al.* 1995b) does not support the hypothesis that restite unmixing could produce the petrological variations in the monzogranite. Quartz is anhedral, interstitial, and some grains contain inclusions of biotite and muscovite, suggesting its late crystallization.

Minor minerals include biotite, muscovite, epidote, and garnet. Magnetite, ilmenite, apatite, zircon, monazite, xenotime, and titanite are accessory minerals, which occur either as inclusions in the major or minor silicate phases, or are interstitial to them

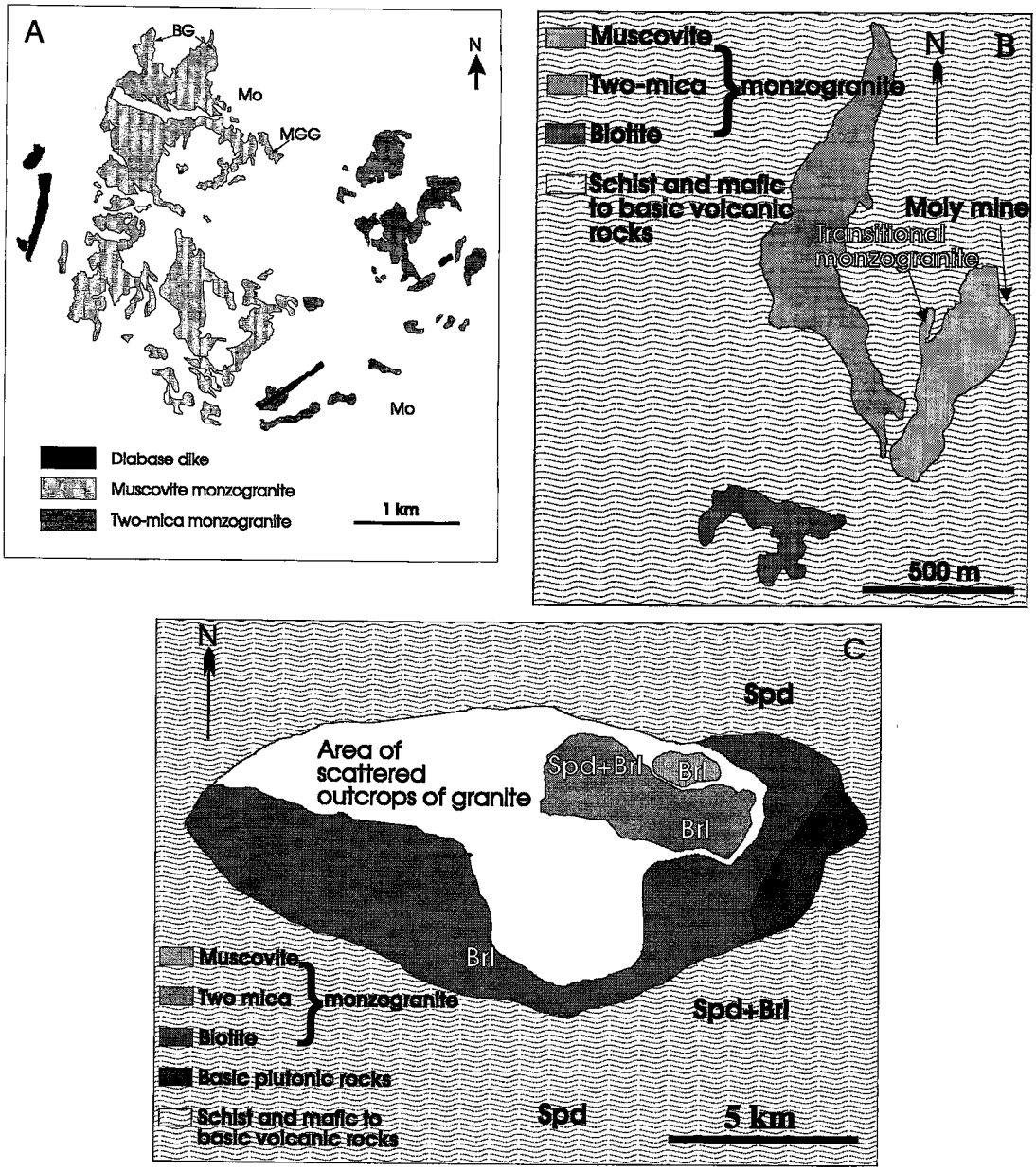

FIGS. 2A, B, C. Geological maps of the Preissac (A), Moly Hill (B) and Lamotte (C) plutons showing the field relationships of the various subtypes of monzogranite and the mineral deposits. In the Preissac pluton, the biotite monzogranite (BG) rims a small part of the muscovite monzogranite in the north, and the muscovite–garnet monzogranite (MGG) occurs as dikes in the northeastern corner of the muscovite monzogranite (details in text). Two former molybdenite mines (Mo) are the Preissac in the north and the Cadillac in the southeast. The biotite monzogranite in the Moly Hill pluton occurs as a small hill, the two-mica monzogranite as a flat-lying outcrop, and the muscovite monzogranite as a crest-like mass. The small body of transitional monzogranite has a mineralogy intermediate between two-mica and muscovite monzogranites. The Lamotte pluton has an asymmetrical normal zonation. A large part of this pluton consists of small granitic outcrops, which define the intrusive boundary. Brl and Spd are beryl- and spodumene-bearing pegmatites, respectively.

(Fig. 3). The distribution of both minor and accessory minerals changes systematically from biotite through two-mica to muscovite monzogranite (Fig. 4). The exceptions to this generalization involve xenotime and ilmenite, which have similar abundances in all subtypes of monzogranite. The contents of biotite, epidote, magnetite, ilmenite, apatite, zircon, monazite, and titanite (which, in some cases, is Nb-bearing) decrease gradually, whereas those of muscovite and garnet increase, from the biotite monzogranite, through the two-mica monzogranite, to the muscovite monzogranite. Molybdenite, columbite–tantalite, and sphalerite were observed only in the muscovite and muscovite–garnet monzogranites and in pegmatites.

Effects of subsolidus fluid–rock interaction are evident in the partial replacement of some crystals of plagioclase and K-feldspar by muscovite, the partial replacement of biotite by chlorite ± ilmenite ± rutile, or epidote, and the presence of perthitic microcline.

The Preissac pluton is exposed as an asymmetrical dome having dips that are steeper to the west and north than to the east and south (Fig. 2A). The pluton is composed mostly of two-mica and muscovite monzogranites, the former ranges from coarse to medium grained, and the latter is generally medium grained in the south and fine grained in the north; these two major outcrops of muscovite monzogranite are separated by a wide fracture (see below). Contacts between the two subtypes of monzogranite are not exposed. At the margins of the pluton, monzogranite lenses locally intermingle with biotite schist, which was recrystallized as a result of contact metamorphism. A subtle foliation has been observed along the northeastern margin, where muscovite in the pluton is oriented parallel to the contact. Fine-grained biotite monzogranite occurs as a thin marginal facies at the northern tip of the pluton, where it grades sharply into the muscovite monzogranite or is separated from the latter by irregular quartz + K-feldspar veins. Dikes (up to 3 m wide) of muscovite–garnet monzogranite, with vugs containing molybdenite and pyrite, intruded the northeastern margin of the pluton (Fig. 2A). The dikes appear to represent the youngest phase of monzogranite-related igneous activity, as they cut both the Mo-bearing quartz veins and pod-shaped pegmatites.

The muscovite monzogranite developed extensive fractures or joints that strike mostly east and southeast with steep dips (Fig. 2A). No slickensides were observed in most of the major fractures. Dawson (1966) suggested that these nearly parallel fractures were formed by tension in a north–south direction. Some of the fractures are occupied by barren pegmatites, and barren and Mo-bearing quartz veins.

Figure 3

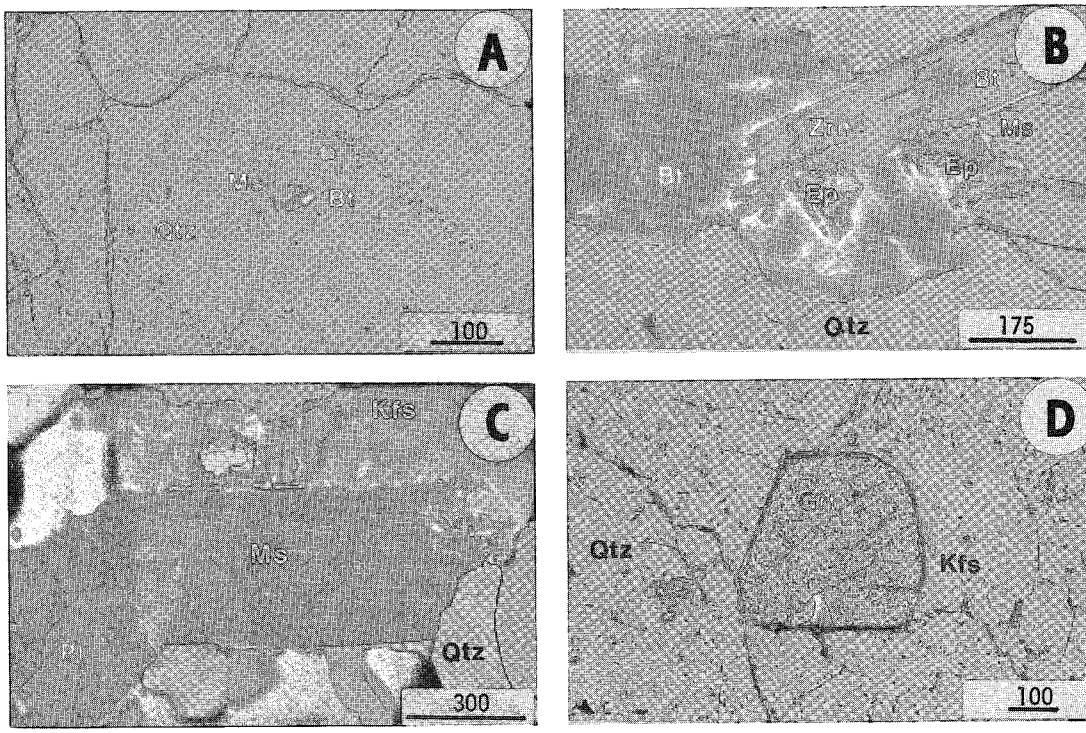

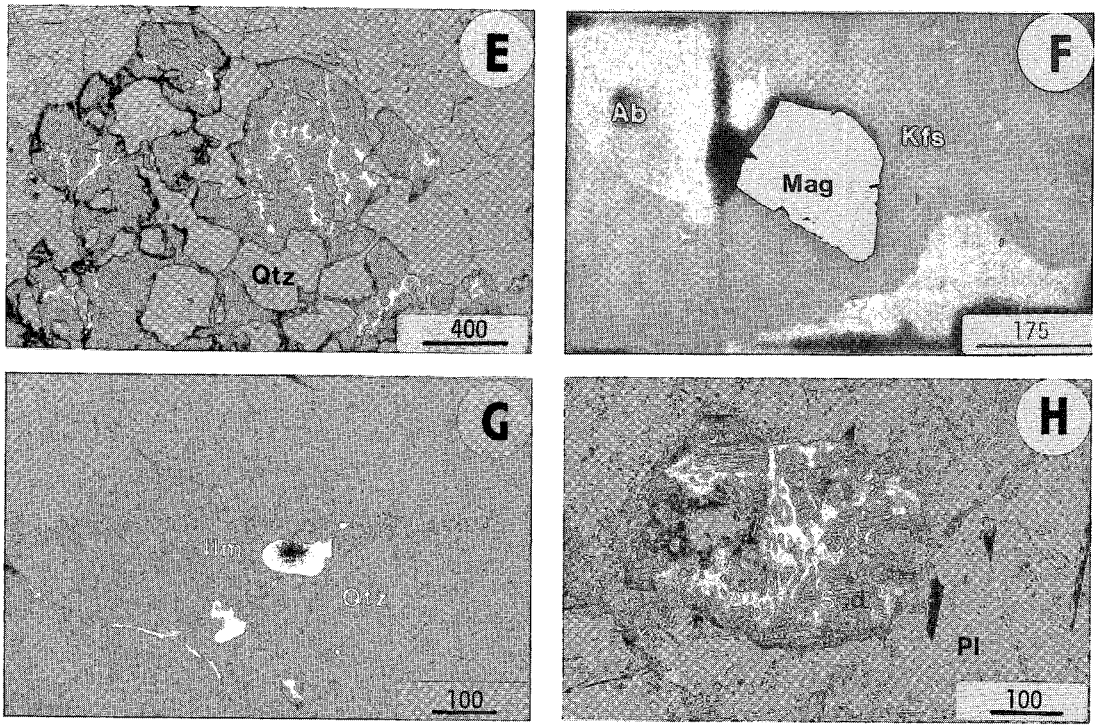

FIG. 3. Photomicrographs of minor and accessory minerals (identity confirmed by scanning electron microscopy with energy-dispersion spectrometry) in the monzogranites. A. Included biotite (Bt) in sharp contact with muscovite (Ms) in quartz (Qtz) (TM–766). To the right of the micas is a plane of fluid inclusions. B. Cross-cutting biotite and muscovite, and interstitial epidote (Ep) (TM–782). Zircon (Zrn) inclusions with halos are present in the micas. Relict biotite is contained in the cross-cutting secondary muscovite (see text for explanation). C. Coarse-grained euhedral magmatic muscovite displaying sharp contacts with the adjacent quartz, plagioclase (Pl) and K-feldspar (Kfs) (TM–652). D. Euhedral interstitial garnet (Grt) in biotite monzogranite (TM–672). E. Anhedral, skeletal garnet intergrown with quartz in two-mica monzogranite located near a fracture (TM–797). F. Subhedral magnetite (Mag) partly enclosed in K-feldspar and adjacent albite (Ab) (TM–40). G. A euhedral inclusion of ilmenite (Ilm) in quartz. Planes of fluid inclusions occur nearby. H. A corroded xenocryst of spodumene enclosed in plagioclase.

Economic molybdenite-bearing quartz veins form a stockwork immediately north of the dikes (Preissac mine), and another close to the southern margin of the pluton (Cadillac mine).

The Moly Hill pluton is exposed in three main separated outcrops, consisting of massive fine- to medium-grained biotite monzogranite, foliated medium-grained two-mica monzogranite and muscovite monzogranite (Fig. 2B). The muscovite monzogranite includes a small body of two-mica monzogranite with gradational contacts. The boundary with the biotite schist in the northern two-mica monzogranite varies from sharp to irregular as a result of randomly oriented networks of quartz veinlets in the monzogranite and biotite schist. At their present level of exposure, the three rock types form a horst-and-graben-like structure, in which the two-mica monzogranite is the down-thrown block. However, a cataclastic texture was not observed in the marginal part of any of three monzogranites, indicating that the field relations among the monzogranites are not due to faults. Instead, thermally metamorphosed biotite schist and basalt occur along the contacts between the two-mica monzogranite and the muscovite monzogranite, and a foliation defined by the micas developed in the two-mica and muscovite monzogranites. The field relationships and mineral fabric suggest that intrusion of the monzogranitic magma was fracture-controlled.

A quartz-vein type of Mo deposit is situated between the eastern margin of the muscovite monzogranite and mafic volcanic rocks. This muscovite monzogranite is finer grained than that in the main mass. Although the mafic rocks are not exposed, their existence can be inferred from inclusions of altered mafic rocks along the walls of subhorizontal quartz veins. Irregularly zoned, east–west-trending pegmatite

and aplite dikes cut the biotite monzogranite.

The Lamotte pluton is asymmetrically zoned, and grades inward from porphyritic to coarse-grained biotite monzogranite at the margin to medium-grained two-mica monzogranite and muscovite monzogranite (Fig. 2C). Contacts between the various subtypes of monzogranite were not observed. The contact with the biotite schist is characterized by complex mixing of aplites and pegmatites in the east, by a concentration of irregular Mo-bearing quartz veins in the south, and by a contact-metamorphic zone containing cordierite, garnet, staurolite and sillimanite in the north (Dawson 1966). Xenoliths of partially digested biotite schist are present along the eastern margin of the two-mica monzogranite.

Samples of biotite and two-mica monzogranite taken near the contact with the biotite schist contain anhedral crystals of spodumene (Fig. 3H) and anhedral aggregates of spodumene, altered biotite, K-feldspar, and quartz. The mode of occurrence of these crystals and aggregates, and disequilibrium textural relationships with other minerals in the rocks, suggest that they are xenocrysts and xenoliths, respectively.

The Lacorne pluton has a north–south-oriented elliptical plan, and is dominated by biotite monzogranite, which gives way inward to two-mica and muscovite monzogranite (Fig. 2D). No contacts between these subtypes of monzogranite were observed, except that between the biotite and two-mica monzogranite in the north, which is gradational; contacts with the biotite schist are sharp. A dike-like muscovite monzogranite intrusion, separated from the main mass by faults, crops out in the southern part of the pluton. The various subtypes of monzogranite are generally medium-grained, except along the northwestern margin, where the biotite monzogranite is fine grained and foliated, and probably represents a chilled margin, and in the east where the discrete two-mica monzogranite (labeled Valor, Fig. 2D) is finer-grained and has a whiter hue. In addition, the dike-like muscovite monzogranite differs from the muscovite monzogranite in the main body by the absence of biotite and a heterogeneous texture. Xenoliths of diorite and biotite schist occur in the pegmatites in the northwest, and in the dike-like muscovite monzogranite in the south, respectively.

Pegmatites and albitites. Over 1600 bodies of barren and mineralized pegmatite have been recorded in the study area (Dawson 1966), and they cut all subtypes of monzogranite and adjacent country-rocks. The pegmatite bodies generally strike east–west and range in dip from vertical to subhorizontal. The mineralogy of the barren pegmatites is similar to that of the muscovite monzogranite, except that biotite is absent and garnet is more abundant. Mineralized or rare-element-bearing pegmatites are associated with the Lamotte and Lacorne plutons and vary from beryl-bearing at the margins of the plutons, to spodumene-bearing in the country rocks (Figs. 2C, D). In addition, the pegmatites host significant amounts of columbite–tantalite, and subordinately, tourmaline and molybdenite.

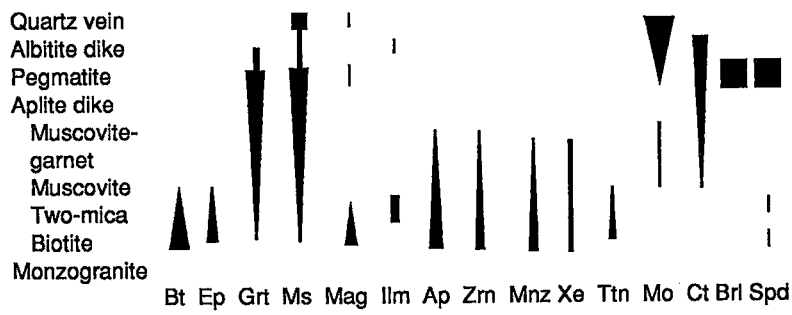

FIG. 4. The paragenesis of minor and accessory minerals commonly found in the monzogranites, pegmatites, albitites and quartz veins. The width of the lines indicates relative abundance (based on point-counting). Symbols: Bt: biotite, Ep: epidote, Grt: garnet, Ms: muscovite, Mag: magnetite, Ilm: ilmenite, Ap: apatite, Zrn: zircon, Mnz: monazite, Xe: xenotime, Ttn: titanite, Mo: molybdenite, Ct: columbite–tantalite, Brl: beryl, Spd: spodumene. Dashed lines for spodumene indicate that the mineral is a xenocryst. Not shown are hematite, which occurs in traces with quartz in veinlets that cut the plutons, allanite in the Lamotte biotite monzogranite, rutile, and tourmaline, pyrophanite ($MnTiO_3$) and gahnite ($ZnAl_2O_4$), which occur as small grains in the pegmatites.

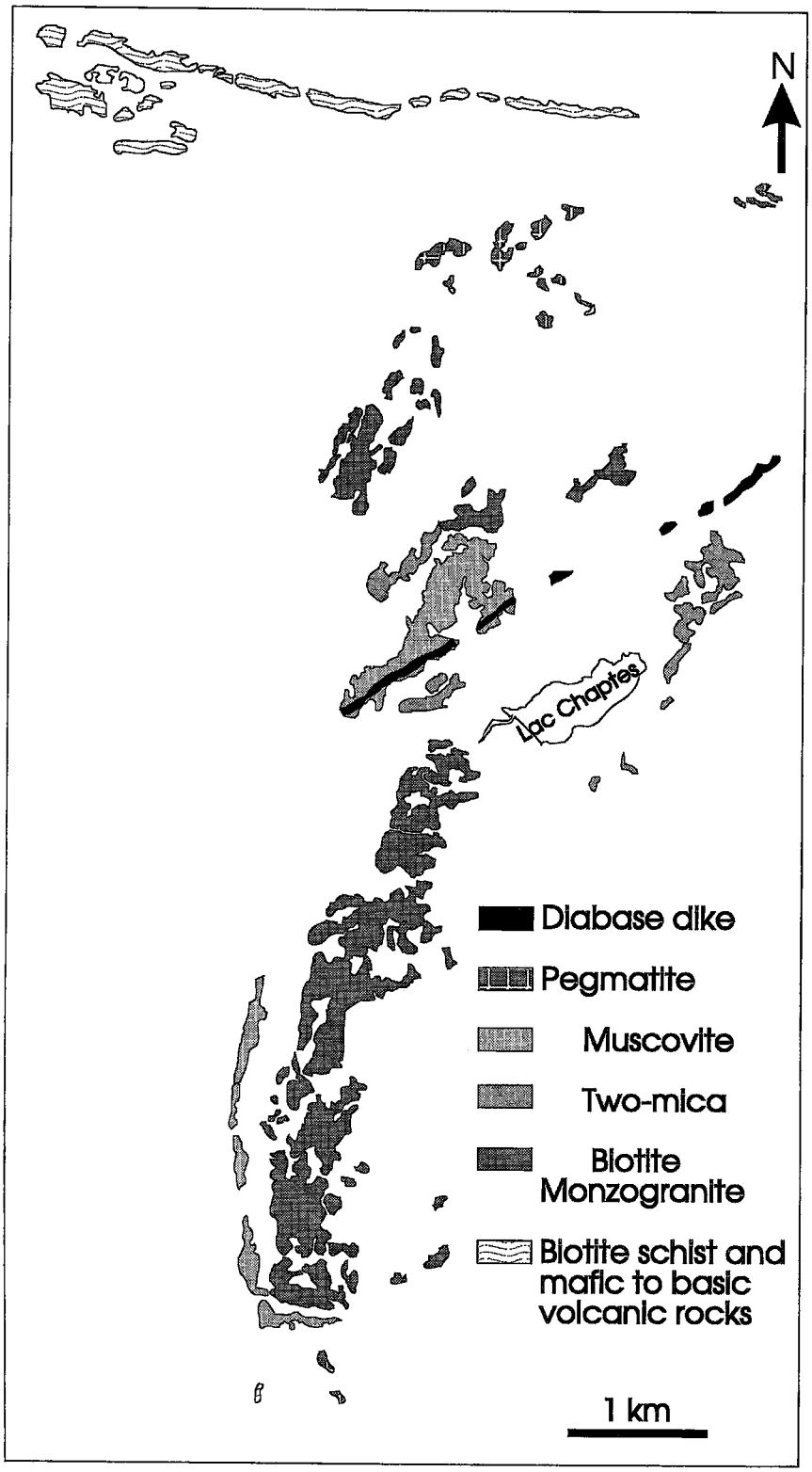

FIG. 2D. A geological map and an aerial (mosaic) photograph of the Lacorne pluton covering the western part of the intrusion, where the main outcrops are exposed. Like the Lamotte pluton, small outcrops of undifferentiated granitic rocks were taken as the boundary of the pluton (Fig. 1). The northern boundary of the biotite monzogranite is a few hundred meters north of the gravel road. The Québec Lithium (QL) mine is about 8 km east of the margin of this photograph. Other spodumene-bearing pegmatites and molybdenite-bearing quartz veins are located about 2.5 km south of the pluton. The northeast-trending diabase dike is shown by dashed lines. Abbreviations are similar to those of Figure 2A; the others shown here are: V, Valor (name of prospect); GD, granodiorite; MG2, muscovite monzogranite dike (details in text); MBP, mass beryl pegmatite; P, pegmatite; AB, albitite dike; SV: biotite schist and mafic volcanic rocks (Abitibi "greenstone" rocks). Mineral symbols: Be, beryl; Spd, spodumene; Mo, molybdenite.

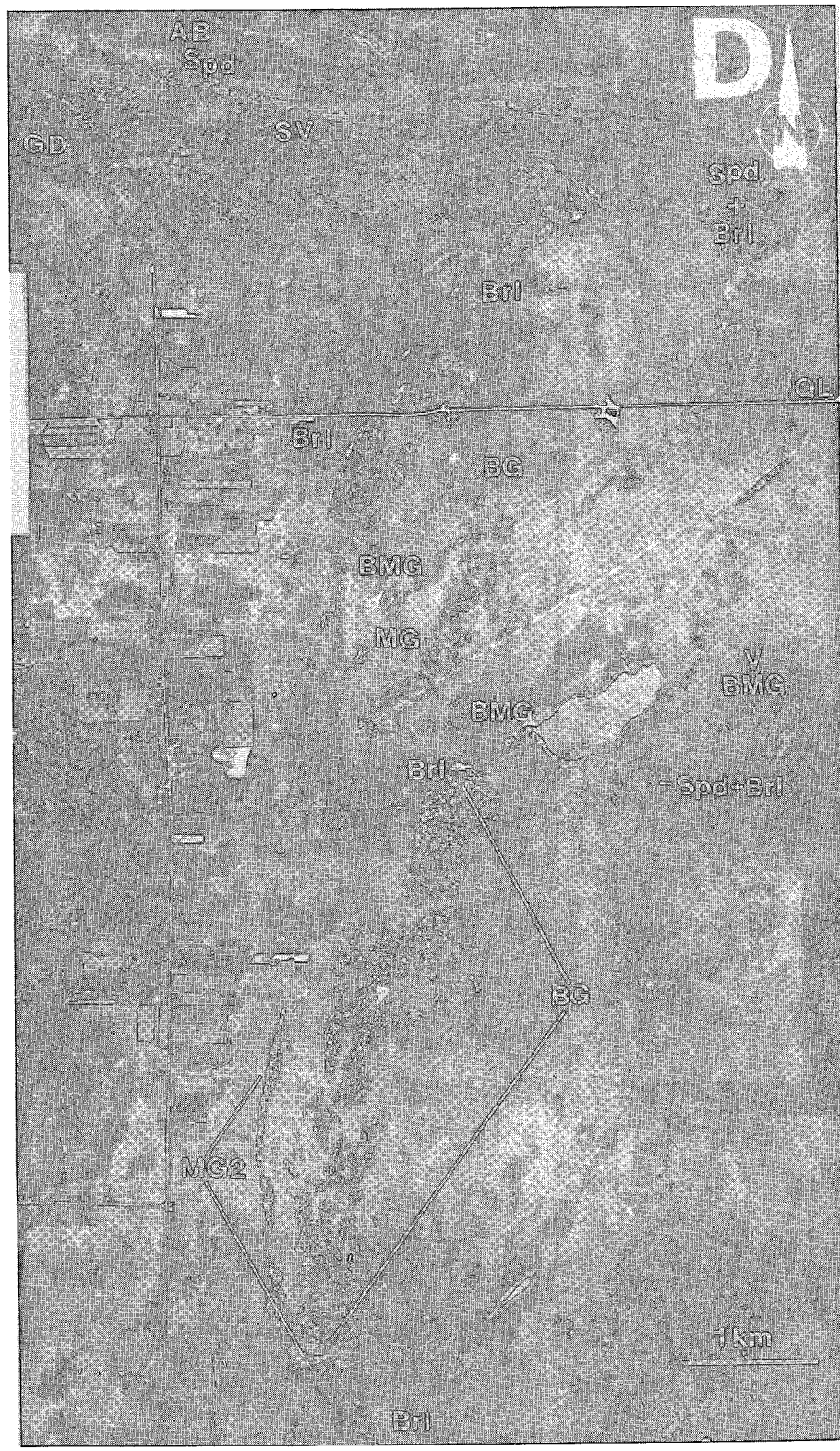
D
AB
Spd
GD
SV
Spd
+
Brl
Brl
QL
Brl
BG
BMG
MG
V
BMG
BMG
Brl
Spd+Brl
BG
MG2
1 km
Brl

The rare-element pegmatites display internal textural variations. A simple zoned pegmatite typically consists of an aplite border-zone and a pegmatite core. In one case, the two units form a layered intrusion, in which each pegmatite consists of an aplite footwall and a pegmatite hanging-wall. Complex beryl pegmatites are typically zoned from the margin to center as follows: (1) border-zone aplite, (2) muscovite + albite + quartz + beryl, (3) perthite + quartz + beryl, (4) perthite + quartz, (5) massive quartz. Spodumene pegmatites, which normally do not contain beryl or have very little beryl, are massive (*i.e.*, without clear internal zonation) or zoned. The latter pegmatites, which display a mineralogical zonation similar to that of the beryl pegmatites, contain spodumene in zones 2 to 5. Transitional spodumene–beryl pegmatite are characterized by the occurrence of beryl crystals at the boundary between zones 1 and 2, the presence of spodumene in zones 2 to 5, and "cleavelandite" and lepidolite in zones 3 and 4.

Molybdenite- and columbite–tantalite-bearing albitite dikes and Mo-bearing quartz veins occur beyond the spodumene pegmatite zone to the north and south of the Lacorne pluton, respectively. The dikes vary from 20 cm to 1 m wide, have an east–west strike (parallel to the joints of the country rocks) and dip steeply (about 75° to the south). They consist almost of entirely of albite (Ab_{99}), appreciable amounts of molybdenite and columbite–tantalite, and traces of zircon and Ta-bearing ilmenite.

Mineral Chemistry

Analytical methods

The compositions of silicate and oxide minerals were determined with an automated CAMECA electron microprobe. The operating conditions were: acceleration voltage 15 kV, beam current 8 nA (10 nA for garnet), a 2-μm spot size (defocused to about 6 μm for feldspar), and counting time 25 seconds (60–75 seconds for fluorine). Standard minerals used were: albite (Na), orthoclase (Al, K, Si), diopside (Ca, Mg), andradite and magnetite (Fe), spessartine (Mn, Si, Al in analyses of garnet), fluorite (F), and synthetic MnTi (Mn, Ti). Data reduction was accomplished with full PAP correction procedures (Pouchou & Pichoir 1984). Muscovite separates were analyzed by Bondar–Clegg Laboratory, Ottawa, for Cs, Ta, Sc, and Rb using instrumental neutron-activation analysis, Li using atomic absorption spectrometry, and F using an ion-selective electrode.

Plagioclase

Plagioclase compositions typically range from An_{15} in the biotite monzogranite to An_7 in the muscovite monzogranite, and less than An_5 in the pegmatites (Table 1, Fig. 5). Exceptions to this are plagioclase phenocrysts in the Lamotte biotite monzogranite, which have a composition of

TABLE 1. REPRESENTATIVE COMPOSITIONS OF PLAGIOCLASE

	Biotite monzogranite				Two-mica monzogranite				Muscovite monzogranite				MGG*
Pluton**	PR	MH	LM	LC	PR	MH	LM	LC	PR	MH	LM	LC	PR
Sample	402	29	782	614	903	31	766	652	302	12	101	684	473
SiO_2	67.28	65.41	65.31	65.07	66.31	66.46	66.1	66.46	67.44	66.05	66.12	66.94	67.45
Al_2O_3	20.35	21.61	22.29	21.43	20.87	20.98	22.11	21.31	20.56	20.89	21.6	20.83	20.27
Na_2O	10.71	9.86	9.51	10.07	10.05	9.95	9.68	10.3	10.81	10.68	10.28	10.45	11.18
K_2O	0.06	0.15	0.2	0.09	0.19	0.13	0.1	0.12	0.14	0.14	0.19	0.07	0.07
CaO	1.38	3.15	3.68	2.75	2.22	3.15	2.33	2.5	1.87	1.31	2.47	1.77	0.97
Total	99.78	100.2	100.9	99.41	99.64	100.7	100.3	100.7	100.8	99.07	100.7	100.1	99.94
Number of cations on the basis of 8 oxygen atoms													
Si	2.949	2.874	2.85	2.879	2.917	2.902	2.885	2.998	2.935	2.919	2.887	2.929	2.953
Al	1.052	1.119	1.463	1.118	1.083	1.08	1.137	1.096	1.055	1.088	1.112	1.074	1.046
Na	0.911	0.84	0.804	0.864	0.858	0.842	0.819	0.872	0.912	0.915	0.870	0.887	0.949
K	0.004	0.008	0.011	0.005	0.011	0.75	0.005	0.007	0.008	0.008	0.010	0.004	0.004
Ca	0.065	0.148	0.172	0.13	0.105	0.147	0.109	0.117	0.087	0.062	0.115	0.083	0.045
End members Mol. %													
Ab	93	84	81.5	86.5	88	84.5	87.7	87.5	90.6	93	87	91	95
Or	0.4	1	1	0.5	1	0.7	0.6	0.7	0.7	1	1	0.5	0.5
An	6.6	15	17.5	13	11	14.8	11.7	11.8	8.7	6	12	8.5	4.5

* Muscovite–garnet monzogranite. ** PR: Preissac, MH: Moly Hill, LM: Lamotte, LC: Lacorne. Oxides reported in weight %.

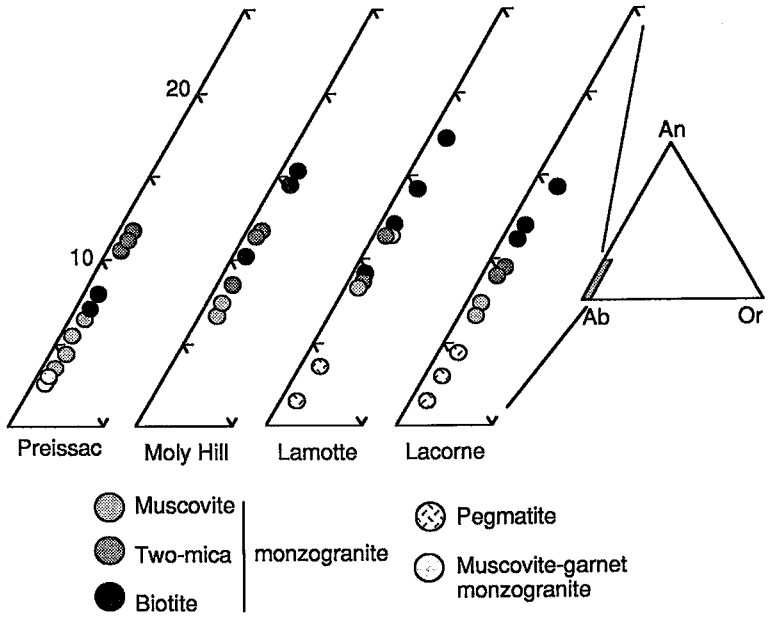

FIG. 5. Molar proportions of albite (Ab), anorthite (An) and orthoclase (Or) in plagioclase.

$An_{17.5}$, and plagioclase in both the biotite monzogranite and muscovite monzogranite of the Preissac pluton, which have compositions of An_8, and An_{3-7}, respectively. Muscovite–garnet monzogranite which, as noted above, occurs only in the Preissac pluton, contains plagioclase of average composition An_3.

In addition to variations in the composition of the plagioclase with the subtype of monzogranite, the composition also varies spatially, *i.e.*, in the Lacorne biotite monzogranite the An content of plagioclase decreases from the margins inward (Fig. 6), and in the Preissac muscovite monzogranite and the Moly Hill two-mica monzogranite, plagioclase generally becomes more sodic northward and eastward, respectively.

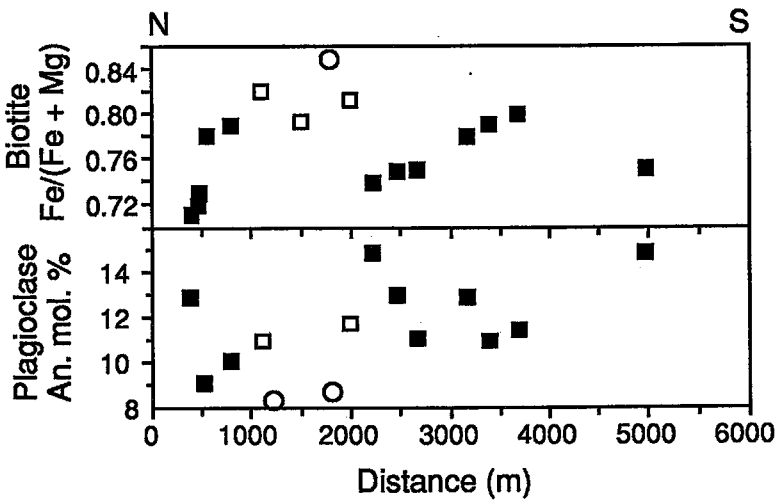

FIG. 6. Compositional variations in plagioclase and biotite along a north–south traverse across the Lacorne monzogranite pluton. Solid square: biotite monzogranite, open square: two-mica monzogranite, and open circle: muscovite monzogranite.

TABLE 2 REPRESENTATIVE COMPOSITIONS OF K-FELDSPAR

	Biotite monzogranite				Two-mica monzogranite				Muscovite monzogranite				MGM**
Pluton*	PR	MH	LM	LC	PR	MH	LM	LC	PR	MH***	LM	LC	1a
Sample	402	29	767	614	903	31	766	652	302	24	101	633	477
SiO_2	64.11	65.13	66	64.65	65.1	65.00	65.33	65.68	65.13	65.05	65.41	64.56	64.30
Al_2O_3	17.94	18.18	18.39	17.96	17.65	17.62	18.44	17.05	17.96	18.30	18.14	17.80	18.15
Na_2O	0.45	0.39	0.40	0.33	0.62	0.36	0.37	0.36	0.34	1.24	0.29	0.41	0.28
K_2O	16.67	17.12	15.90	16.99	16.66	17.11	16.73	16.78	16.89	15.86	17	16.79	16.97
CaO	0.09				0.01			0.01					
Total	99.26	100.8	100.7	99.93	100	100.1	101	99.88	100.3	100.40	100.8	99.56	99.70
Number of cations on the basis of eight oxygen atoms													
Si	2.997	3.000	3.016	3.003	3.015	3.012	2.999	3.044	3.009	2.993	3.005	3.008	2.992
Al	0.989	0.987	0.991	0.983	0.964	0.962	0.998	0.931	0.978	0.992	0.982	0.977	0.996
Na	0.041	0.035	0.035	0.030	0.055	0.033	0.033	0.032	0.031	0.111	0.026	0.037	0.026
K	0.994	1.006	0.927	1.007	0.985	1.012	0.980	0.992	0.996	0.931	1.000	0.998	1.007
Ca	0.004	0.000	0.000	0.000	0.001	0.000	0.000	0.001	0.000	0.000	0.000	0.000	0.000
End members Mol. %													
Ab	4	3.4	4	3	5	3	3	3	3	11	2.5	3.6	2.5
Or	95.5	96.6	96	97	95	97	97	97	97	89	97.5	96.4	97.5
An	0.5												

* Pluton headings as in Table 1. ** Muscovite–garnet monzogranite. *** Including albite lamellae. Oxides reported in weight %.

K-feldspar

As noted earlier, the K-feldspar is perthitic. K-feldspar domains in perthite have a narrow range of composition, from $Or_{95}Ab_4An_1$ to $Or_{98}Ab_2$ (Table 2), and do not show any significant compositional variations with rock type, sample location, or paragenesis. Most contain less than 0.1 wt.% CaO. Broad beam (10 μm) analyses of perthite including the albite lamellae yielded a composition of $Or_{89}Ab_{11}$ (Sample 24, Table 2). The high Or-content of the K-feldspar and the perfection of the degree of order Al–Si (R.F. Martin, pers. comm., 1995) indicate that it re-equilibrated at postmagmatic conditions.

Biotite

Biotite is either early, forming inclusions in quartz, and to a lesser extent, feldspar, or late, occurring in interstices between the major silicate phases (Figs. 3A–B). Compositionally, it has a higher Fe/(Fe + Mg) value, in the range from 0.69 to 0.85, and is less aluminous (^{IV}Al: 2.1–2.5 atoms per formula unit, apfu) than biotite in other peraluminous granites (data compiled by Clarke 1981). The atomic proportions of Si–ΣAl–M^{2+} (M^{2+}: Fe + Mg + Mn) show that it has a significant content of a dioctahedral component, which is higher in the interstitial biotite than in the included biotite (Fig. 7). In the Lamotte and Lacorne biotite monzogranites, the included biotite is consistently lower in SiO_2, TiO_2 and Al_2O_3, generally lower in Na_2O, and invariably higher in $FeO_{(t)}$ than the interstitial variety (Table 3), and has similar ranges of MnO,

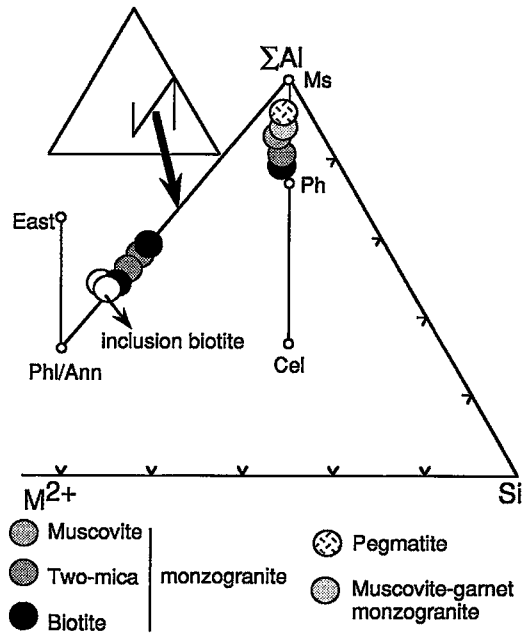

FIG. 7. Average compositions of biotite and muscovite for each of the subtypes of monzogranite and pegmatite, plotted in atomic proportions of ΣAl–M^{2+}–Si (diagram after Monier & Robert 1986). Although the plot suggests dioctahedral–trioctahedral substitution in the biotite, and Al-Tschermak substitution for the muscovite, the absence of Li analyses precludes corroboration of the mechanism of exchange. M^{2+}: Fe + Mn + Mg. East: eastonite, Phl/Ann: phlogopite/annite, Ms: muscovite, Ph: phengite, Cel: celadonite.

TABLE 3. REPRESENTATIVE COMPOSITIONS OF BIOTITE

	Biotite monzogranite							Two-mica monzogranite							MG*
Pluton	PR	PR	MH	LM	LM	LC	LC	PR	MH	MH	LM	LM	LC	LC	LC
Sample	402**	402+	29	768*	908	613	673+	903	26	41**	766	791**	672+	672	648+
SiO_2	36.37	35.89	36.81	34.76	38.84	37.76	36.91	37.00	36.85	35.86	38.29	38.22	35.42	36.87	37.13
TiO_2	2.58	2.90	2.71	2.43	1.33	1.79	2.45	2.80	2.20	2.86	1.16	1.05	2.12	2.00	1.93
Al_2O_3	16.76	16.39	16.57	17.83	20.03	21.43	17.99	17.07	17.94	16.85	18.63	20.24	17.22	19.64	18.72
FeO	25.33	25.92	23.72	25.3	20.62	19.15	23.24	22.31	23.15	23.00	21.18	20.46	26.41	23.81	22.84
MnO	0.89	0.95	0.60	0.68	0.61	0.80	1.09	0.77	0.94	2.26	1.02	0.7	0.76	0.60	0.68
MgO	4.15	3.89	6.02	4.89	3.29	2.66	4.07	5.40	4.13	4.78	4.74	3.69	3.15	2.91	2.22
Na_2O	0.14	0.02	0.09	0.02	0.01	0.01	0.03	0.04	0.06	0.05	0.04	0.06	0.02	0.05	0.06
K_2O	9.84	10.05	9.90	9.3	9.81	10.08	9.73	10.24	9.63	9.70	9.13	9.9	10.02	10.13	9.81
F	0.69	0.62	0.83	0.72	0.93	1.02	0.96	1.34	0.77	0.51	0.9	0.77	0.97	0.51	1.23
	96.75	96.63	97.25	95.93	95.47	94.70	96.47	96.97	95.67	95.87	95.09	95.09	96.09	96.52	94.62
F=O	0.29	0.26	0.35	0.30	0.39	0.43	0.4	0.56	0.32	0.21	0.38	0.32	0.41	0.21	0.52
Total	96.46	96.37	96.90	95.63	95.08	94.27	96.07	96.41	95.35	95.66	94.71	94.77	95.68	96.31	94.10
	Number of cations on the basis of 22 oxygen atoms														
Si	5.680	5.647	5.674	5.481	5.932	5.801	5.718	5.719	5.739	5.621	5.900	5.864	5.657	5.696	5.853
^{iv}Al	2.320	2.353	2.327	2.519	2.068	2.199	2.282	2.281	2.261	2.379	2.100	2.136	2.343	2.304	2.147
^{vi}Al	0.765	0.687	0.684	0.795	1.537	1.681	1.003	0.829	1.032	0.735	1.284	1.523	0.878	1.239	1.33
Ti	0.303	0.343	0.314	0.277	0.153	0.206	0.285	0.325	0.258	0.338	0.134	0.121	0.253	0.232	0.229
Fe	3.308	3.411	3.057	3.336	3.633	2.461	3.011	2.884	3.016	3.016	2.729	2.625	3.505	3.075	3.011
Mn	0.118	0.126	0.078	1.149	0.749	0.104	0.144	0.101	0.124	0.301	1.090	0.844	0.102	0.078	0.091
Mg	0.966	0.912	1.383	0.091	0.078	0.610	0.939	1.244	0.958	1.116	0.133	0.091	0.745	0.670	0.521
Na	0.043	0.007	0.027	0.005	0.004	0.003	0.009	0.013	0.017	0.016	0.011	0.016	0.006	0.014	0.018
K	1.961	2.016	1.947	1.870	1.911	1.976	1.922	2.020	1.914	1.939	1.795	1.937	2.018	1.996	1.973
F	0.339	0.309	0.404	0.359	0.447	0.490	0.471	0.653	0.381	0.255	0.437	0.376	0.487	0.251	0.614
FM	0.77	0.79	0.69	0.97	0.98	0.80	0.76	0.70	0.76	0.73	0.95	0.97	0.82	0.82	0.85

Pluton headings as in Table 1. * muscovite–garnet monzogranite. + included biotite. " included biotite coexisting with muscovite.
** Coexists with muscovite. FM: Fe/(Fe + Mg). Oxides reported in weight %.

MgO and K_2O, and F. As a result, there is a slight overlap in the Fe/(Fe + Mg) value of biotite, which ranges from 0.69–0.76 in interstitial biotite to 0.72–0.80 in included biotite. This is opposite to the compositional behavior of biotite in the Cuffytown Creek pluton, South Carolina, where the interstitial biotite has the higher Fe/(Fe + Mg) value (Speer & Becker 1992). A trend of decreasing Fe/(Fe + Mg) of biotite during crystallization of plutonic rocks is common (*e.g.*, Czamanske & Wones 1973, Chivas 1981, Parsons 1981), and is attributed to an increase in the oxygen fugacity and a drop in temperature. According to these authors, the increasing oxidation is caused by the increased partial pressure of water, which is enhanced by higher amounts of fluid exsolved from the crystallizing magma.

Included biotite is rare in the two-mica monzogranites of the Lamotte and Lacorne plutons, and analyses are too few to permit meaningful comparisons with those of interstitial biotite. Therefore, unless otherwise stated, the following discussion refers to interstitial biotite.

The Fe/(Fe + Mg) of biotite in the Moly Hill, Lamotte and Lacorne plutons increases from approximately 0.69 in the biotite monzogranite to 0.85 in the muscovite monzogranite. However, this trend is reversed in the Preissac monzogranites, with the Fe/(Fe + Mg) ratio decreasing from approximately 0.78 in the biotite monzogranite to 0.69 in the two-mica monzogranite. Within the biotite monzogranite of the Lamotte pluton, this ratio generally increases toward the two-mica monzogranite. This trend is also observed in the northern part of the Lacorne pluton. In the southern body of biotite monzogranite in this pluton, however, the Fe/(Fe + Mg) value of the biotite increases toward the center of the mass (Figs. 2D, 6). There is no apparent trend in the Fe/(Fe + Mg) value of biotite in the biotite monzogranite of the Moly Hill pluton, and no trend can be determined for this ratio in the Preissac pluton, because the biotite monzogranite occurs only as a narrow marginal facies.

The fluorine content of biotite in both biotite and two-mica monzogranites has a similar range, from 0.6 to 1.4 wt.%, except for the Preissac pluton, where the F content varies very little and averages 0.65 and 1.35 wt.% in the two rock types, respectively. The average F content of biotite in the biotite monzogranite is marginally higher than that of biotite in the two-mica monzogranite of the Moly Hill, Lamotte, and Lacorne plutons (0.93 *versus* 0.78 wt.%).

Muscovite

On the basis of textural relationships, muscovite can be subdivided into primary and secondary varieties (*cf.* Miller *et al.* 1981, Speer 1984). Primary muscovite forms discrete, randomly distributed euhedral crystals, many of which are similar in size to other major silicate phases (Fig. 3C). Less commonly, such muscovite occurs as inclusions in quartz. The primary muscovite is characterized by its higher Ti and Na contents and lower Mg content than secondary muscovite, which has a composition similar to hydrothermal muscovite in quartz veins (this study). Secondary muscovite occurs mostly as cross-cutting grains containing relics of biotite, intergrowths of ilmenite or rutile, and inclusions of zircon (Fig. 3B). Muscovite in the muscovite and biotite monzogranites is dominantly primary and secondary, respectively. In contrast, both varieties of muscovite are common in the two-mica monzogranite. Muscovite in the pegmatites occurs as large books concentrated mostly near the contact with the host monzogranite or with aplitic phases in the pegmatites.

The atomic proportions of Si–ΣAl–M^{2+}(M^{2+}: Fe + Mg + Mn) in the primary muscovite in the different subtypes of monzogranite suggest that the muscovite becomes progressively less phengitic and approaches the end-member composition in the muscovite monzogranite and the pegmatites (Fig. 7). As with biotite, the Fe/(Fe + Mg) of muscovite increases from 0.65 to 0.85 from the biotite monzogranite to the muscovite monzogranite and pegmatite (Table 4). The fluorine content of muscovite ranges from <0.3 to 1.6 wt.%; the lower value is considered to represent the detection limit of F using the electron microprobe. The most F-enriched muscovite occurs in the Lacorne biotite monzogranite and has an average of 0.8 wt. % F. There is, moreover, a clear trend of decreasing average F content of muscovite from biotite through two-mica (0.6 wt.%) to muscovite monzogranite (0.4 wt.%). The muscovite in the monzogranites of the other plutons has significantly less F, but nevertheless also displays trends of decreasing F content from biotite or two-mica to muscovite monzogranite (Preissac: 0.45, <0.3, <0.3; Moly Hill: <0.3, 0.55, 0.4; Lamotte: 0.52, 0.54, 0.36). Somewhat surprisingly, this trend is not continued into the pegmatites; muscovite in these rocks shows a wide range of F contents (Lamotte, <0.3 to 1.0 wt.%; Lacorne <0.3 to 2.1 wt.%).

Lithium, which was only sought in muscovite from pegmatites and in two samples of muscovite monzogranite (one each from the Lamotte and Lacorne

TABLE 4. REPRESENTATIVE COMPOSITIONS OF PRIMARY MUSCOVITE

	Biotite monzogranite				Two-mica monzogranite				Muscovite monzogranite				MGG**
Pluton	PR	MH	LM	LC	PR	MH	LM	LC	PR	MH	LM	LC	PR
Sample	402*	29	782*	613	902	32	791	652	302	17	101	648	479
SiO_2	46.93	46.67	47.30	46.85	47.24	46.46	47.63	48.49	46.95	46.49	46.78	46.01	46.75
TiO_2	0.91	1.77	0.23	0.40	0.97	0.61	0.12	0.27	0.62	0.43	0.3	0.34	0.22
Al_2O_3	27.82	27.39	29.38	28.49	28.87	30.49	31.35	31.35	27.14	30.83	31.14	31.43	31.47
FeO	6.11	5.84	5.07	7.77	5.58	5.06	4.10	4.66	6.21	5.27	3.7	5.28	5.22
MnO	0.11	0.14	0.11	0.36	0.10	0.17	0.1	0.09	0.15	0.06	0.05	0.10	0.12
MgO	1.45	1.50	1.62	1.09	1.42	0.92	1.41	1.06	1.73	0.71	0.68	0.72	0.71
Na_2O	0.15	0.23	0.26	0.06	0.23	0.34	0.21	0.23	0.20	0.22	0.3	0.37	0.31
K_2O	11.38	11.49	10.93	10.04	11.44	11.44	10.79	10.19	11.25	11.52	11.12	11.34	11.02
F		0.71	0.53	1.20		1.59							
		95.74	95.43	96.26		97.08							
O-F=O		0.30	0.22	0.51		0.67							
Total	94.86	95.44	95.21	95.75	95.85	96.41	95.71	96.34	94.25	95.53	96.41	95.59	95.82
	Number of cations based on 22 oxygen atoms												
Si	6.484	6.446	6.468	6.453	6.439	6.246	6.406	6.462	6.534	6.344	6.271	6.276	6.335
^{iv}Al	1.516	1.554	1.532	1.547	1.561	1.754	1.594	1.538	1.466	1.656	1.729	1.724	1.665
^{vi}Al	3.013	2.908	3.205	2.713	3.078	3.078	3.376	3.385	2.985	3.303	3.507	3.328	3.360
Ti	0.095	0.185	0.024	0.041	0.100	0.062	0.012	0.027	0.064	0.045	0.028	0.035	0.022
Fe	0.706	0.675	0.58	0.895	0.636	0.569	0.461	0.519	0.723	0.601	0.415	0.602	0.591
Mn	0.013	0.016	0.012	0.042	0.012	0.019	0.011	0.010	0.018	0.007	0.006	0.012	0.014
Mg	0.298	0.310	0.33	0.224	0.288	0.184	0.282	0.211	0.359	0.144	0.137	0.146	0.143
Na	0.039	0.062	0.069	0.016	0.060	0.089	0.056	0.060	0.053	0.058	0.078	0.098	0.082
K	2.005	2.025	1.906	1.764	1.990	1.962	1.852	1.732	1.998	2.006	1.902	1.973	1.905
F		0.310	0.23	0.523		0.676							

Pluton headings as in Table 1. Fluorine concentration less than 0.4 wt.% is not listed. * Cross-cutting bith biotite. Oxides reported in weight %.

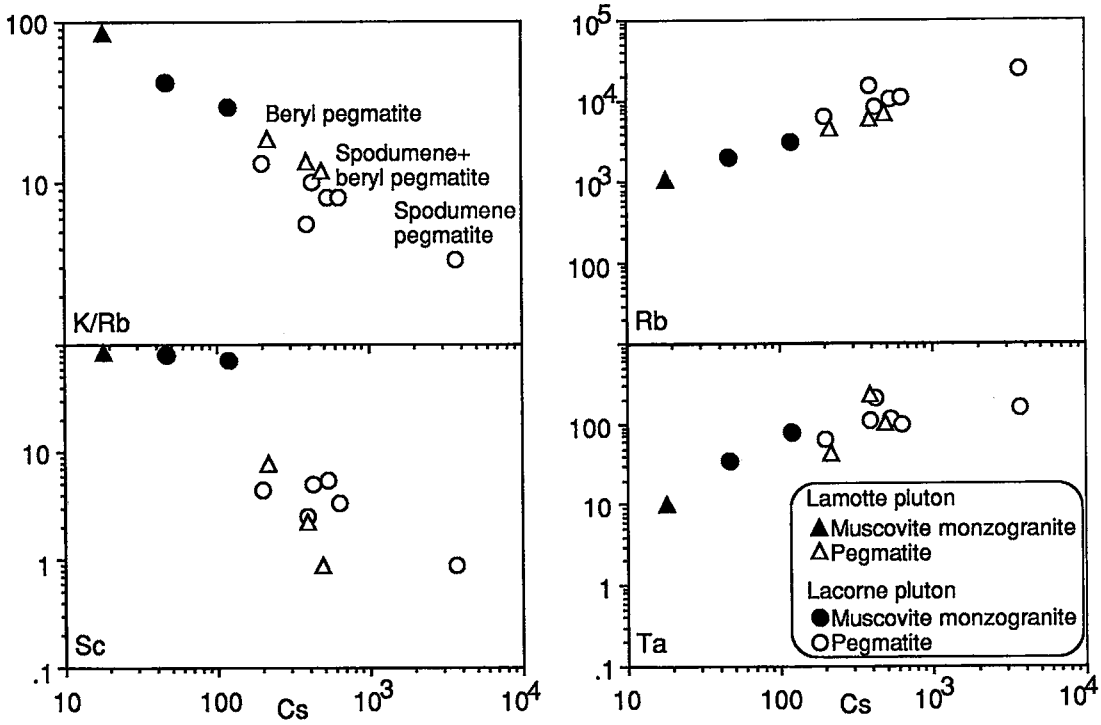

FIG. 8. Plots illustrating the variations of K/Rb, Sc, Rb and Ta with Cs in muscovite. The muscovite samples from the pegmatites are from border zones, along which the mineral occurs as cumulate-like aggregates, with the exception of sample HP9–5 (Table 5), where it is disseminated throughout the pegmatite. The sample with the highest Cs content is lepidolite, which was collected from a spodumene pegmatite in the Lacorne pluton.

TABLE 5. TRACE ELEMENT CONTENTS OF MUSCOVITE SEPARATES (ppm)

LAMOTTE PLUTON					
Host rock	MG	Be	Be	Li + Be	Li
Sample No.	101*	912	798	TMC-2	HP9-5
ppm					
Cs	18	213	n.a	234	497
Sc	84	7.7	2.2	1.6	0.9
Ta	10	44	n.a	57	103
Rb	1080	4620	6230	9040	7300
Li	2060	5365	1690	4030	1520
F	2050	9630	5430	7140	875

LACORNE PLUTON								
Host rock	MG	MG	Be	Be	Be + Li	Li + Be	Li + Be	Li
Sample No.	648*	633*	952	1008	753	708	711	756**
ppm								
Cs	46	120	200	422	390	532	632	3680
Sc	83	72	4.4	5	2.5	5.5	3.4	0.9
Ta	35	78	64	207	110	113	98	160
Rb	2100	3100	6540	8290	14900	10600	10700	24600
Li	2890	n.a	1520	1090	990	12400	3730	27500
F	3376	2804	2797	2804	1697	11220	7245	20780

Host rock. MG: muscovite monzogranite; Be, Li: beryl, spodumene pegmatite
*Samples 101 and 648 contain small amounts of biotite, whereas Sample 633 has none.
**Lepidolite

plutons), shows a strong positive correlation with F. The Li_2O content of muscovite in the muscovite monzogranite samples is 0.4 and 0.6 wt. %. The Cs content of muscovite from the muscovite monzogranite and rare-metal pegmatites in the Lamotte and Lacorne plutons correlates positively with Ta and Rb, and negatively with Sc and K/Rb (Table 5, Fig. 8).

Garnet

Garnet forms small, randomly distributed, euhedral to subhedral interstitial crystals and anhedral aggregates or clots concentrated near fractures and quartz veins (Figs. 3D–E). The first mode of occurrence suggests magmatic crystallization, whereas the second mode of occurrence is interpreted to reflect a subsolidus origin; the texture resembles that of metasomatic garnet described by Kontak & Corey (1988) from monzogranite in the South Mountain Batholith, Nova Scotia.

The primary garnet is a spessartine–almandine solid solution ($Sps_{30-60}Alm_{59-37}$; Table 6), which in most cases is normally zoned, *i.e.*, Mn content decreases

TABLE 6. REPRESENTATIVE COMPOSITIONS OF GARNET

	Biotite monzogranite			Two-mica monzogranite				Muscovite monzogranite			MGG	Aplite	Peg
Pluton	LM		LC	MH	LM	LM	LC	PR	MH	LC	PR	MH	LC
Sample	797		631	35	796	907	672	314	17	637	473	30	1001
	core	rim	n=6			n=4				n=4			
SiO_2	37.00	36.85	36.6	36.17	36.80	36.97	36.87	36.27	36.70	36.56	35.83	36.31	36.63
Al_2O_3	19.69	19.66	20.15	20.13	20.30	20.50	19.80	19.96	20.43	19.57	20.00	20.31	19.89
TiO_2	0.29	0.19		0.14			0.12		0.11		0.16		
FeO	21.89	25.72	19.75	17.52	28.72	25.96	20.50	20.58	20.18	19.39	16.37	21.08	18.25
Fe_2O_3	1.26	1.36	0.70	0.68			1.05	0.61		1.27	1.19		0.80
MgO	0.55	0.42	0.42	0.28	0.49	0.34	0.51	0.23	0.29	0.24	0.16	0.30	0.11
MnO	18.32	15.07	20.62	23.99	13.05	15.55	19.87	20.66	20.87	20.24	26.14	20.33	23.29
CaO	1.30	1.28	1.73	1.11	0.67	1.00	0.78	0.66	1.14	1.75	0.75	1.30	0.38
Total	100.3	100.5	99.97	100	100	100.3	99.50	98.97	99.72	99.02	100.6	99.63	99.35
				Number of cations based on 24 oxygen atoms									
Si	6.073	6.056	6.021	5.977	6.029	6.049	6.091	6.040	6.017	6.079	5.928	5.979	6.062
Al	3.809	3.808	3.961	3.921	3.919	3.953	3.855	3.917	4.001	3.835	3.904	3.942	3.879
Ti	0.036	0.024		0.017			0.015		0.014		0.020		
Fe^{2+}	3.004	3.535	2.718	2.422	3.935	3.547	2.832	2.866	2.794	2.696	2.265	2.903	2.525
Fe^{3+}	0.156	0.169	0.088	0.058			0.130	0.760		0.159	0.149		0.100
Mg	0.135	0.103	0.103	0.069	0.120	0.083	0.126	0.057	0.072	0.060	0.040	0.073	0.026
Mn	2.550	2.098	2.874	3.358	1.811	2.155	2.781	2.914	2.934	2.851	3.663	2.834	3.264
Ca	0.229	0.225	0.305	0.197	0.118	0.175	0.138	0.118	0.203	0.332	0.133	0.230	0.068
				End members Mol. %									
Alm	51	59	45	40	66	59	48	48	47	46	37	48	43
Prp	2	2	2	1	2	1	2	1	1	1	1	1	0
Grs			3	1		2			3	1		2	
Adr	4	4	2	3	2	1	2	2	0	4	2	2	1
Sps	43	35	48	56	30	36	47	49	49	48	60	47	56

Pluton headings as in Table 1. Peg: pegmatite. n: number of analyses. Oxides reported in weight %.

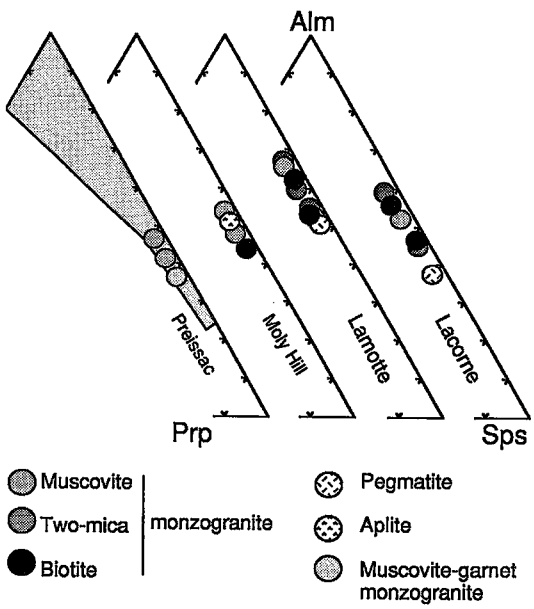

toward the rim; less than 5% of the garnet crystals analyzed are reversely zoned. In both types of garnet, the average variation in Mn is 4 wt.% MnO. Primary and secondary garnets in the monzogranites are indistinguishable on the basis of the major-element compositions, whereas secondary garnets in pegmatite are strongly enriched in Mn (85–90 mol.% Sps). The primary garnet in most of the monzogranites has a wide range in composition, but only in the Preissac pluton is there any evidence of systematic change in garnet composition with subtype of monzogranite; the garnet in the muscovite–garnet monzogranite is richer in Mn than that in the muscovite monzogranite (Fig. 9).

FIG. 9. Compositions of garnet recalculated to 100 mol.% in terms of end-members almandine (Alm), pyrope (Prp), and spessartine (Sps). The shaded area shows the range of garnet compositions compiled by Clarke (1981) for other peraluminous granites.

Epidote

Coarse-grained, euhedral to subhedral crystals of epidote are invariably intergrown with biotite or chloritized biotite, and the contacts between the two minerals vary from sharp to corroded (Fig. 3B). Smaller grains replaced plagioclase and muscovite. Epidote that replaced biotite is richer in ferric iron than epidote that replaced plagioclase or muscovite; the atomic ratio $Fe^{3+}/(Fe^{3+} + Al)$ varies from 0.26 to 0.33 *versus* 0.22 to 0.24, respectively (Table 7). Epidote from biotite schist in contact with the Preissac two-mica monzogranite has a consistent $Fe^{3+}/(Fe^{3+} + Al)$ ratio of 0.24. The higher ratio, according to Naney (1983) and Tulloch (1979), reflects a magmatic origin, and the lower ratio, a hydrothermal origin. On textural grounds, we conclude that epidote in the Preissac–Lacorne monzogranites is secondary, and that the $Fe^{3+}/(Fe^{3+} + Al)$ value depends simply on the nature of the mineral replaced, *i.e.*, we do not believe that this chemical criterion can be used to distinguish primary from secondary epidote. This opinion is supported by data for epidote in granitic rocks from Nova Scotia and the southern Appalachians. There, the epidote is believed to be magmatic on textural grounds, yet its $Fe^{3+}/(Fe^{3+} + Al)$ ratio ranges from 0.23 to 0.29 (Farrow & Barr 1992), and from 0.24 to 0.33 (Vyhnal *et al.* 1991), respectively.

Iron–titanium oxides and titanite

The composition of magnetite does not vary from one monzogranite subtype to the next, and is very close to Fe_3O_4. Primary and secondary crystals of ilmenite have essentially the same composition, and contain significant amounts of Mn (from 4 to 11.5 wt.% MnO). In the albitite dikes, this mineral contains up to 1.2 wt.% Ta_2O_5. Neither magnetite nor ilmenite hosts any exsolved phases (Figs. 3F–G). The primary titanite contains very little or negligible amounts of Mn, higher Si and lower Ti than secondary titanite. The latter, together with chlorite, replaced biotite. The primary titanite crystals contain minor levels of niobium.

TABLE 7. REPRESENTATIVE COMPOSITIONS OF EPIDOTE

Host rock	BG			2MG					MG	BG	MG	SC
Pluton	LM	LC	LC	PR	MH	LM	LC	LC	PR	LC	LC	
Sample	908	613	620	902	26	791	673	707	302	614	603	921
Texture	1	1	1	2	1	1	1	2	2	3	4	1
SiO_2	38.10	38.44	38.32	39.23	38.06	38.00	38.05	38.30	38.88	39.57	39.20	38.76
TiO_2	0.12	1.16	0.30		0.13	0.22		0.19				
Al_2O_3	22.26	22.31	21.83	23.68	22.77	22.48	21.69	22.58	23.00	23.79	24.83	23.85
Fe_2O_3	13.68	12.86	14.40	12.78	13.16	14.10	15.20	13.44	13.34	11.72	10.95	11.52
MnO	0.26	0.46	0.25	0.61	0.61	0.23	0.27	0.46	0.45	0.85	0.16	0.31
CaO	23.05	22.67	22.10	22.52	22.37	23.05	22.77	22.77	22.53	22.17	22.98	22.15
Total	97.47	97.90	97.20	98.82	97.10	98.08	97.98	97.74	98.20	98.10	98.12	96.59
Number of cations based on 13 oxygen atoms												
Si	3.051	3.177	3.197	3.297	3.277	3.029	3.163	3.176	3.303	3.237	3.196	3.214
Ti	0.007	0.072	0.019		0.008	0.013		0.012				
Al	2.101	2.174	2.147	2.345	2.311	2.110	2.126	2.207	2.304	2.294	2.387	2.331
Fe^{3+}	0.825	0.800	0.904	0.809	0.853	0.845	0.951	0.839	0.853	0.721	0.672	0.719
Mn	0.017	0.032	0.018	0.043	0.044	0.016	0.019	0.032	0.033	0.059	0.011	0.022
Ca	1.978	2.008	1.974	2.028	2.064	1.967	2.028	2.023	2.050	1.943	2.008	1.968
▲	0.28	0.27	0.30	0.26	0.27	0.28	0.31	0.28	0.27	0.24	0.22	0.24

▲▲ $Fe^{3+}/(Fe^{3+} + Al)$

Pluton headings as in Table 1. Host rock: BG: biotite monzogranite, 2MG: two-mica monzogranite, MG: muscovite monzogranite, SC: schist. Texture: 1: coexists with biotite and feldspar, 2: coexists with primary muscovite, 3: interstitial, 4: replacing plagioclase. Oxides reported in weight %.

Discussion

Evolution of the AFM minerals

We have used the parageneses and compositions of the AFM mineral assemblages (biotite, muscovite, garnet) in the various subtypes of the monzogranite and the corresponding AFM liquidus topologies of Abbott (1985) to trace the reactions believed to have taken place during the course of crystallization of the monzogranitic magma (*cf.* Speer & Becker 1992) (Figs. 10A, B).

The presence of included biotite in the Lamotte and Lacorne biotite monzogranite suggests the reaction liquid → Bt. In contrast, evidence for contemporaneous crystallization of included biotite and muscovite in the Preissac two-mica monzogranite and in the Moly Hill biotite monzogranite indicate that the liquid of these intrusions was on the three-phase surface, liquid–Bt–Ms, precipitating the two micas by the reaction liquid → Bt + Ms. The final assemblage in the Moly Hill biotite monzogranite consisted of biotite and muscovite, indicating that the reaction continued until the consolidation of the monzogranite (Fig. 10B).

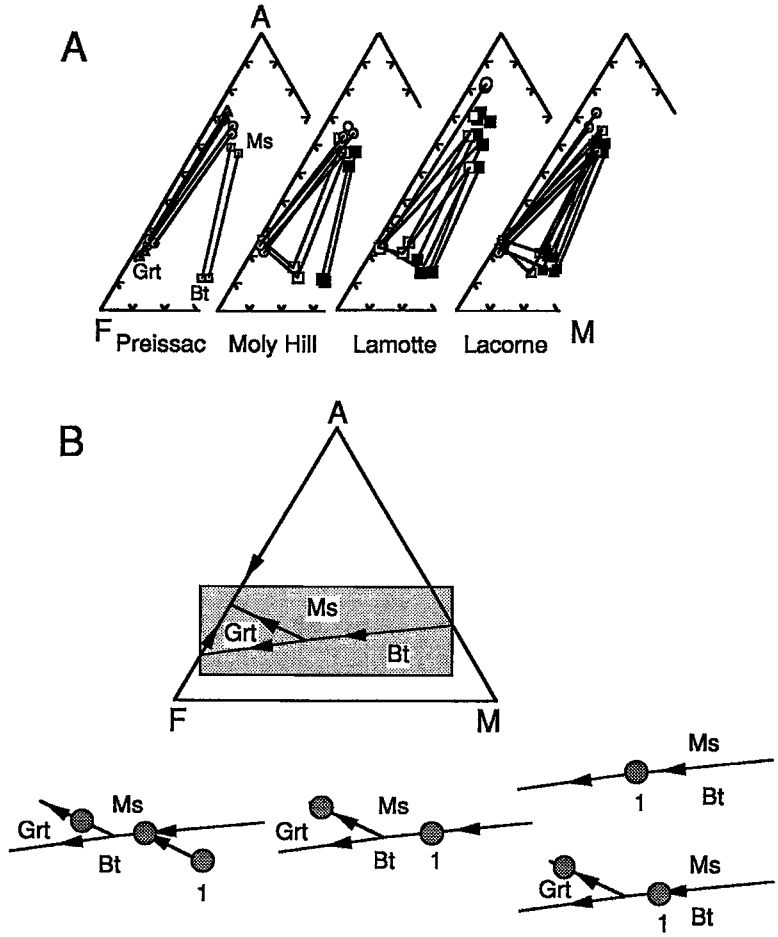

FIG. 10. Compositions of the liquidus AFM minerals (biotite, muscovite, garnet) plotted on an A (Al_2O_3–CaO–Na_2O–K_2O) – F (FeO + MnO) – M (MgO) triangular diagram (A), and the corresponding liquidus AFM diagram [B, after Abbott (1985)]. Coexisting minerals are indicated by tie lines. Solid square: biotite monzogranite, open square: two-mica monzogranite, open circle: muscovite monzogranite, triangle: muscovite–garnet monzogranite (Preissac pluton only). The initial composition of the liquid is indicated by the number 1, and the paths of the crystallization are shown with arrows.

After the included micas had formed in the Preissac, Lamotte and Lacorne plutons, the liquid crystallized the more abundant interstitial biotite and isolated muscovite. The final AFM minerals to crystallize were muscovite and garnet. The appearance of late garnet was a consequence of the crystallization of the micas and Mn-poor magnetite, which increased the Mn/(Mn + Fe + Mg) of the liquid, because of the intolerance of biotite for high levels of Mn^{2+} (Abbott 1985).

The occurrence of Ms + Grt suggests that the remaining liquid only moved onto the Ms + Grt cotectic surface from the three-phase cotectic, liquid + Bt + Ms, through the four-phase peritectic, liquid + Bt + Ms + Grt. There is no evidence to indicate whether the reaction, liquid → Bt + Ms + Grt, or liquid + Bt + Ms → Grt, occurred. It thus follows that after crystallization of biotite, the final liquid must have been on the Ms + Grt cotectic surface, precipitating both minerals by the reaction, liquid → Ms + Grt, until the final consolidation of the monzogranitic magma.

In conclusion, crystallization of the monzogranites in the Preissac–Lacorne plutons proceeded by the same sequence of reactions: liquid → Bt, liquid → Bt + Ms, liquid → Ms + Grt, with the exception of the Moly Hill biotite monzogranite and Preissac muscovite monzogranite, in which crystallization involved only one reaction, liquid → Bt + Ms, and liquid → Ms + Grt, respectively.

P–T conditions of crystallization

As mentioned earlier, Powell *et al.* (1994) have estimated the pressure of contact metamorphism around the Preissac–Lacorne batholith to be about 3.5 kbar. We have accordingly assumed this to be the pressure of emplacement of the monzogranites. A minimum estimate of the pressure is 2.1 kbar, which corresponds to the lower-pressure limit of stability of the assemblage spodumene + quartz (London 1984). The muscovite–biotite (Hoisch 1989), garnet–biotite (Williams & Grambling 1990), and plagioclase – K-feldspar (Brown & Parsons 1981) geothermometers all yield similar temperatures in the range 320–450°C, which clearly indicate subsolidus conditions (Table 8). Probable magmatic temperatures were obtained from the monazite and zircon "geothermometers", which are based on the solubility of these minerals in the magma (Rapp *et al.* 1987, Watson & Harrison 1983). The geothermometers yield temperatures of 685 and 780°C, respectively, in the biotite monzogranite, and 670 and 720°C, respectively, in the muscovite monzogranite.

TABLE 8. INFERRED TEMPERATURE OF CRYSTALLIZATION BASED ON OXYGEN ISOTOPE AND SATURATION OF MONAZITE AND ZIRCON

Pluton	Mineral pair	Temperature in °C			
		Biotite	Two-mica monzogranite	Muscovite	Vein
Preissac	Δqtz-ms				514-576
	Δqtz-grt		695		
	Monazite	nc	680		
	Zircon	nc	765	750	
Moly Hill	Δqtz-ms				540-595
	Δqtz-grt			580	
	Monazite	690	700	675	
	Zircon	777	750	730	
Lamotte	Monazite	680	680	670	
	Zircon	780	740	660	
Lacorne	Monazite	685	670	665	
	Zircon	780	750	750	

qtz: quartz, grt: garnet, ms: muscovite
Source of data: Preissac vein (Taner 1989); Moly Hill vein (Mulja et al. 1990); others (Feng 1992)
nc: not calculated owing to the altered nature of the rock (described in text).

The higher temperature given by the zircon "geothermometer" can be attributed to the fact that zircon is one of the earliest minerals to crystallize, *i.e.*, the 780°C temperature is probably close to that of the liquidus of the monzogranitic magma. The lower temperature indicated for the monazite "geothermometer" reflects crystallization closer to the solidus or *LREE* undersaturation of the melt (Scaillet *et al.* 1990). This deduction is consistent with the parageneis of monazite, which occurs mostly as an interstitial phase. Th lower temperature is, moreover, similar to the temperature of 695°C estimated for oxygen isotopic fractionation between paragenetically late magmatic quartz and garnet in the two-mica monzogranite of the Preissac pluton. A minimum estimate of the solidus temperature is provided by the quartz–muscovite ^{18}O fractionation in a quartz vein from the Moly Hill pluton (Table 8). The temperature is about 40°C lower than that experimentally determined for H_2O-saturated granite by Johannes & Holtz (1991). Although experimental studies by Manning (1981) and Martin (1983) showed that F and Li lower the liquidus and solidus temperatures of granitic melts (*e.g.*, 35°C with 1 wt.% F and 25°C with 1 wt.% Li_2O), this would not have been a factor for the Preissac–Lacorne monzogranites, which contain low levels of F and Li, 0.05 and 0.1 wt.%, respectively (Mulja *et al.* 1995b).

Thus, in summary, the above data suggest that the monzogranitic magma in the Preissac–Lacorne batholith crystallized over the interval 750 to 650°C and a pressure of 3.5 kbar.

Processes controlling monzogranite crystallization and emplacement

From the data presented above, it is clear that the biotite monzogranite is the least differentiated and the muscovite monzogranite the most differentiated of the principal intrusive phases in the Preissac–Lacorne plutons. In going from biotite to muscovite monzogranite, there is a change in mineralogy from biotite to garnet, oligoclase to albite, and niobium-bearing

titanite to columbite–tantalite. Parallel with these mineralogical changes, the An content of plagioclase decreases, the Fe/(Fe + Mg) of biotite increases, and the Al content of muscovite increases. The only exception to this is found in the Preissac pluton, where the biotite monzogranite is anomalous relative to the other subtypes of monzogranite. As mentioned earlier, the biotite monzogranite occurs there only as a thin marginal facies of the muscovite monzogranite, and the extent of the map unit is unknown. Its contacts with the muscovite monzogranite are sharp in some localities and are separated by quartz + K-feldspar veins in others. These field relationships imply two separate pulses of magma. However, owing to the absence of cross-cutting relationships, the sequence of intrusion is not known. The Preissac biotite monzogranite is therefore excluded from the following discussion.

In the Lamotte pluton and, to a lesser extent, in the Lacorne pluton, there is a clear inward zonation from biotite monzogranite (least evolved) to muscovite monzogranite (most evolved) in the core. Similar zonal distributions of intrusive facies have been documented for a number of granitic intrusions, *e.g.*, the Tuolumne Intrusive Series, California (Bateman & Chappell 1979), the Blue Tier batholith, Tasmania (McCarthy & Groves 1979), and the Loch Doon pluton, Scotland (Tindle & Pearce 1981), and in each of these intrusions the sequence of crystallization was from a marginal biotite facies to a muscovite-bearing facies. These spatial and temporal relationships have been interpreted as evidence for side-wall fractional crystallization as the main mechanism of fractionation. Whereas we believe that the process of fractional crystallization also explains various mineralogical and petrological characteristics of the monzogranite plutons in the Preissac–Lacorne batholith, we do not consider that this mechanism was restricted to side-wall crystallization. The spatial trends of Fe/(Fe + Mg) of biotite and An content of plagioclase within the Lacorne pluton suggest that the direction of crystallization was not uniform (Fig. 6). Independent side-wall crystallization seems to have taken place from both ends of the pluton.

The Preissac and Moly Hill plutons are not concentrically zoned. However, the variations in mineralogy and mineral chemistry are similar to those observed in the Lamotte and Lacorne plutons. Moreover, in the case of the Moly Hill pluton, there is a gradual transition from the two-mica monzogranite to the muscovite monzogranite. Gradual transitions from one subtype of monzogranite to another also are observed in the northern part of the Lacorne pluton, where the biotite monzogranite grades imperceptibly into two-mica monzogranite. Such transitions are consistent with the model of fractional crystallization proposed above.

In all four plutons, biotite was the earliest AFM mineral to crystallize, thereby lowering the magma in Mg/(Mg + Fe) and in F. Such depletions are documented by the increase in the Fe/(Fe + Mg) ratio and decrease in the F content of biotite, from biotite monzogranite to two-mica monzogranite, and the decrease in Ti from included to interstitial biotite. They are also documented by similar trends of Fe/(Fe + Mg) and F for muscovite in going from two-mica to muscovite monzogranite. Early biotite was accompanied by crystallization of the most calcic plagioclase (oligoclase), which served to deplete the magma in Ca. The crystallization of biotite and oligoclase led to higher Fe/(Fe + Mg) and Na/(Na + K) values, thereby promoting the crystallization of muscovite, garnet, and sodic plagioclase (albite).

Although the process of fractional crystallization is supported by the geochemistry of the monzogranite (Mulja *et al.* 1995b) and the preceding paragraphs have stressed the importance of gradational boundaries between monzogranite subtypes, many of the contacts are fracture-bounded or unexposed, and at least one, between muscovite–garnet monzogranite and muscovite monzogranite (Preissac pluton), is clearly intrusive. The two-mica monzogranite in the northeastern part of the Lacorne pluton (labeled Valor) differs texturally from, and has an uncertain spatial relationship to, the two-mica monzogranite in the main mass (Fig. 2D). Thus, the muscovite–garnet monzogranite and the Valor two-mica monzogranite in the Preissac and Lacorne plutons, respectively, are likely to represent different pulses of magma.

Relationships between monzogranite and rare-element pegmatites

The most evolved members of the plutons are the pegmatites, which are characterized by plagioclase with the lowest An content, muscovite with the highest Al content, the most spessartine-rich garnet, and the absence of biotite. Trace-element contents of the muscovite, considered from the muscovite monzogranite to various subtypes of rare-element pegmatite, form a systematic trend that suggests a petrogenetic linkage between the two rock types (Table 5, Fig. 8). These trends are consistent with a process of differentiation in which the residual liquid is progressively enriched in Cs, Rb, and Ta, and depleted in Sc. This, in turn, suggests that the muscovite monzogranite and pegmatites are comagmatic. The above trends are also evident among the different types of rare-element pegmatites, *i.e.*, beryl-bearing pegmatites have higher K/Rb, Sc, and lower Cs, Rb, and Ta contents than spodumene-bearing pegmatites; these components have intermediate concentrations in the spodumene + beryl-bearing pegmatites. This interpretation is corroborated by the chemical composition of columbite–tantalite, which evolved from ferrocolumbite in beryl pegmatite to manganotantalite in spodumene pegmatites (Mulja *et al.* 1995a), and by the whole-rock geochemistry of the pegmatites

(Mulja *et al.* 1995b). Therefore, the residual melts from fractional crystallization of the monzogranitic magma continued to differentiate to form the pegmatites.

Conclusions

1. The monzogranitic plutons (Preissac, Moly Hill, Lamotte, Lacorne) of the Preissac–Lacorne batholith were emplaced at a pressure of 3.5 kbar, and crystallized over a temperature range from 750 to 650°C.
2. These plutons vary from biotite through two-mica to muscovite monzogranite subtypes, which display gradational, intrusive, and fracture-bounded contacts.
3. Field relations and systematic mineralogical and mineral-chemical variations within and between the monzogranite subtypes are interpreted to have been produced mainly by fractional crystallization, and subordinately by intrusion of different batches of magma. The former process caused the early fractionation of oligoclase, biotite and Fe–Ti oxides, and the later crystallization of albite, garnet and muscovite.
4. The end stage of fractional crystallization was marked by the occurrence of beryl, spodumene and columbite–tantalite in pegmatites.

Acknowledgements

This study was supported by a FCAR team grant, a MERQ contract, and NSERC operating grants to A.E. Williams-Jones and S.A. Wood, and a NATO travel grant to S.A. Wood and A.E. Williams-Jones. Field work was assisted by D. Ahmad and A. Fournier. The Ministère de l'Energie et des Ressources (Quebec) kindly permitted us to reproduce their airphotos. We thank P. Černý, F. Holtz, C. Miller, J. Bourne, D. Kontak, R.F. Martin, and an anonymous reviewer for their constructive criticisms and corrections, which improved the manuscript.

References

Abbott, R.N Jr. (1985): Muscovite-bearing granites in the AFM liquidus projection. *Can. Mineral.* **23**, 553-561.

Bateman, P.C. & Chappell, B.W. (1979): Crystallization, fractionation, and solidification of the Tuolumne Intrusive series, Yosemite National Park, California. *Geol. Soc. Am., Bull.* **90**, 465-482.

Breaks, F.W. & Moore, J.M., Jr. (1992): The Ghost Lake batholith, Superior Province of northwestern Ontario: a fertile, S-type, peraluminous granite – rare-element pegmatite system. *Can. Min.* **30**, 835-875.

Brown, W.L. & Parsons, I. (1981): Towards a more practical two-feldspar geothermometer. *Contrib. Mineral. Petrol.* **76**, 369-377.

Černý, P., Goad, B.E., Hawthorne, F.C. & Chapman, R. (1986): Fractionation trends of the Nb- and Ta-bearing oxide minerals in the Greer lake pegmatitic granite and its pegmatite aureole, southeastern Manitiba. *Am. Mineral.* **71**, 501-517.

Chappell, B.W., White, A.J.R. & Wyborn, D. (1987): The importance of residual source material (restite) in granite petrogenesis. *J. Petrol.* **28**, 1111-1138.

Chivas, A. R. (1981): Geochemical evidence for magmatic fluids in porphyry copper mineralization. I. Mafic silicates from the Koloula igneous complex. *Contrib. Mineral. Petrol.* **78**, 389-403.

Clarke, D.B. (1981): The mineralogy of the peraluminous granites: a review. *Can. Mineral.* **19**, 3-17.

Corfu, F. (1993): The evolution of the southern Abitibi Greenstone Belt in light of precise U–Pb geochronology. *Econ. Geol.* **88**, 1323-1340.

Czamanske, G.K. & Wones, D.R. (1973): Oxidation during magmatic differentiation, Finnmarka complex, Oslo area, Norway. 2. The mafic silicates. *J. Petrol.* **14**, 349-380.

Dawson, K.R. (1966): A comprehensive study of the Preissac–Lacorne batholith, Abitibi county, Quebec. *Geol. Surv. Can., Bull.* **142**.

Dimroth, E., Imreh, L., Goulet, N. & Rocheleau, M. (1983): Evolution of the south-central segment of the Archean Abitibi belt, Quebec. III. Plutonic and metamorphic evolution and geotectonic model. *Can. J. Earth. Sci.* **20**, 1374-1388.

Farrow, C.E.G. & Barr, S.M. (1992): Petrology of high-Al-hornblende- and magmatic-epidote-bearing plutons in the southeastern Cape Breton highlands, Nova Scotia. *Can. Mineral.* **30**, 377-392.

Feng, Rui (1992): *Tectonic Juxtaposition of the Archean Greenstone Belt and Pontiac Sub-Province: Evidence from Geobarometry, Geochemistry, and Ar-Ar Geochronology of Metasedimentary Rocks and Granitoids.* Ph.D. thesis, Univ. of Saskatchewan, Saskatoon, Saskatchewan.

_____ & Kerrich, R. (1991): Single zircon age constraints on the tectonic juxtaposition of the Archean Abitibi Greenstone Belt and Pontiac Subprovince, Quebec, Canada. *Geochim. Cosmochim. Acta* **55**, 3437-3441.

_____ & _____ (1992): Geochemical evolution of granitoids from the Archean Abitibi southern volcanic zone and the Pontiac Subprovince, Superior Province, Canada: implications for tectonic history and source regions. *Chem. Geol.* **98**, 23-70.

Gariépy, C. & Allègre, C.J. (1985): The lead isotope geochemistry and geochronology of late kinematic intrusives from the Abitibi Greenstone Belt and the implications for late Archean crustal evolution. *Geochim. Cosmochim. Acta* **49**, 2371-2383.

GOAD, B.E. & ČERNÝ, P. (1981): Peraluminous pegmatitic granites and their pegmatite aureoles in the Winnipeg River district, southeastern Manitoba. *Can. Mineral.* **19**, 177-194.

HOISCH, T.H. (1989): A muscovite–biotite geothermometer. *Am. Mineral.* **74**, 565-572.

JOHANNES, W & HOLTZ, F. (1991): Formation and ascent of granitic magmas. *Geol. Rundsch.* **80**, 225-231.

KONTAK, D.J. & COREY, M. (1988): Metasomatic origin of spessartine-rich garnet in the South Mountain Batholith, Nova Scotia. *Can. Mineral.* **26**, 315-334.

LONDON, D. (1984): Experimental phase equilibria in the system $LiAlSiO_4$–SiO_2–H_2O: a petrogenetic grid for lithium-rich pegmatites. *Am. Mineral.* **69**, 995-1004.

MANNING, D.A.C (1981): The effects of fluorine on liquidus phase relationships in the system Qz–Ab–Or with excess water at 1 kbar. *Contrib. Mineral. Petrol.* **76**, 206-215.

MARTIN, J.S. (1983): An experimental study of the effects of lithium on the granite system. *Proc. Ussher Soc.* **5**, 417-420.

MCCARTHY, T.S. & GROVES, D.I. (1979): The Blue Tier Batholith, Northeastern Tasmania, a cumulate-like product of fractional crystallization. *Contrib. Mineral. Petrol.* **71**, 193-209.

MILLER, C.F., STODDARD, E.F., BRADFISH, L.J., & DOLLASE, W.A. (1981): Composition of plutonic muscovite: genetic implications. *Can. Mineral.* **19**, 25-34.

MONIER, G. & ROBERT, J.-L. (1986): Muscovite solid solutions in the system K_2O–MgO–FeO–Al_2O_3–SiO_2–H_2O: an experimental study at 2 kbar PH_2O and comparison with natural Li-free white micas. *Mineral. Mag.* **50**, 257-266.

MULJA, T., WILLIAMS-JONES, A.E., BOILY, M. & WOOD, S.A. (1990): A geological and fluid inclusion study of the Moly Hill deposit in the Preissac – Lacorne plutonic complex, northwestern Quebec. *Geol. Assoc. Can. – Mineral. Assoc. Can., Program Abstr.* **15**, A93.

———, ———, MARTIN, R.F. & WOOD, S.A. (1995a): Compositional variation and structural state of columbite–tantalite in rare-metal granitic pegmatites of the Preissac–Lacorne batholith, Quebec, Canada. *Am. Mineral.* (in press).

———, ———, WOOD, S.A. & BOILY, M. (1995b): The rare-element-enriched monzogranite – pegmatite – quartz vein systems in the Preissac–Lacorne batholith, Quebec. II. Geochemistry and petrogenesis. *Can. Mineral.* **33**, 817-833.

NANEY, M.T. (1983): Phase equilibria of rock-forming ferromagnesian silicates in granitic systems. *Am. J. Sci.* **283**, 993-1033.

PARSONS, I. (1981): The Klokken gabbro–syenite complex, South Greenland: quantitative interpretation of mineral chemistry. *J. Petrol.* **22**, 233-260.

POUCHOU, J.L. & PICHOIR, F. (1984): A new model for quantitative X-ray microanalyses. I. Application to the analysis of homogeneous samples. *La Recherche Aérospatiale* **3**, 13-38.

POWELL, W.G., CARMICHAEL, D.M. & HODGSON, C.J. (1994): Conditions and relative timing of metamorphism during the evolution of the southern Abitibi Greenstone Belt. *Geol. Assoc. Can. – Mineral. Assc. Can., Program Abstr.* **19**, A90.

RAPP, R.P. & WATSON, E.B. (1986): Monazite solubility and dissolution kinetics: implications for the thorium and light rare earth chemistry of felsic magmas. *Contrib. Mineral. Petrol.* **94**, 304-316.

SCAILLET, B., FRANCE-LANORD, C. & LE FORT, P. (1990): Badrinath–Gangotri plutons (Garhwal, India): petrological and geochemical evidence for fractionation processes in a high Himalayan leucogranite. *J. Volc. Geotherm. Res.* **44**, 163-188.

SHEARER, C.K., PAPIKE, J.J. & JOLLIFF B.L. (1992): Petrogenetic links among granites and pegmatites in the Harney Peak rare-element granite–pegmatite system, Black Hills, South Dakota. *Can. Mineral.* **30**, 785-809.

———, ——— & LAUL, J.C. (1987): Mineralogical and chemical evolution of a rare-earth granite–pegmatite system: Harney Peak granite, Black Hills, South Dakota. *Geochim. Cosmochim. Acta* **51**, 473-486.

SIMMONS, W.B., LEE, M.T. & BREWSTER, R.H. (1987): Geochemistry and evolution of the south Platte granite–pegmatite system, Jefferson County, Colorado. *Geochim. Cosmochim. Acta* **51**, 455-471.

SPEER, J.A. (1984): Micas in igneous rocks. *In* Micas (S.W. Bailey, ed.). *Rev. Mineral.* **13**, 299-356.

——— & BECKER, S.W. (1992): Evolution of magmatic and subsolidus AFM mineral assemblages in granitoids rocks: biotite, muscovite, and garnet in the Cuffytown Creek pluton, South Carolina. *Am. Mineral.* **77**, 821-833.

STEIGER, R.H. & WASSERBURG, G.J. (1969): Comparative U–Th–Pb systematics in 2.7×10^6 yr. plutons of different geologic histories. *Geochim. Cosmochim. Acta* **33**, 1213-1232.

SUTCLIFFE, R.H., BARRIE, C.T., BURROWS, D.R. & BEAKHOUSE, G.P. (1993): Plutonism in the southern Abitibi Subprovince: a tectonic and petrogenetic framework. *Econ. Geol.* **88**, 1359-1375.

TANER, H. (1989): *The Nature, Origin and Physicochemical Controls of Hydrothermal Mo–Bi Mineralization in the Cadillac and Preissac Deposits, Quebec.* M.Sc. thesis, McGill Univ., Montreal, Quebec.

TINDLE, A.G. & PEARCE, J.A. (1981): Petrogenetic modeling of in situ fractional crystallization in the zoned Loch Doon pluton, Scotland. *Contrib. Mineral. Petrol.* **78**, 196-207.

TULLOCH, A.J. (1979): Secondary Ca–Al silicates as low-grade alteration products of granitoid biotite. *Contrib. Mineral. Petrol.* **69**, 105-117.

VYHNAL, C.R., MCSWEEN, H.Y., JR. & SPEER, J.A. (1991): Hornblende chemistry in southern Appalachian granitoids: implications for aluminum hornblende thermobarometry and magmatic epidote stability. *Am. Mineral.* **76**, 176-188.

WALL, V.J., CLEMENS, J.D. & CLARKE, D.B. (1987): Models for granitoid evolution and source composition. *J. Geol.* **6**, 731-749.

WATSON, E.B. & HARRISON, T.M. (1983): Zircon saturation revisited: temperature and composition effects in a variety of crustal magma types. *Earth Planet. Sci. Lett.* **64**, 295-304.

WILLIAMS, M.L. & GRAMBLING, J.A. (1990): Manganese, ferric iron, and the equilibrium between garnet and biotite. *Am. Mineral.* **75**, 886-908.

Received May 26, 1993, revised manuscript accepted June 14, 1994.